

The 3D Cosmic Shoreline for Nurturing Planetary Atmospheres

ZACH K. BERTA-THOMPSON ¹, PATCHARAPOL WACHIRAPHAN ¹ AND CATRIONA MURRAY ¹

¹University of Colorado Boulder, Department of Astrophysical and Planetary Sciences

ABSTRACT

Various “cosmic shorelines” have been proposed to delineate which planets have atmospheres. The fates of individual planet atmospheres may be set by a complex sea of growth and loss processes, driven by unmeasurable environmental factors or unknown historical events. Yet, defining population-level boundaries helps illuminate which processes matter and identify high-priority targets for future atmospheric searches. Here, we provide a statistical framework for inferring the position, shape, and fuzziness of an instellation-based cosmic shoreline, defined in the three-dimensional space of planet escape velocity, planet bolometric flux received, and host star luminosity. We circumvent the need to estimate individual host stars’ historical X-ray and extreme ultraviolet fluences by including luminosity in the definition of the shoreline, explicitly modeling how sharply such drivers of atmospheric escape intensify toward lower-luminosity M dwarf stars and marginalizing over the associated uncertainties. Using Solar System and exoplanet atmospheric constraints, under the assumption that one planar boundary applies across a wide parameter space, we find the critical flux threshold for atmospheres scales with escape velocity with a power-law index of $p = 5.9_{-0.43}^{+0.61}$, steeper than the canonical literature slope of $p = 4$, and scales with stellar luminosity with a power-law index of $q = 1.17_{-0.20}^{+0.28}$, steep enough to disfavor atmospheres on Earth-sized planets out to the habitable zone for stars less luminous than $\log_{10}(L_{\star}/L_{\odot}) = -2.23_{-0.21}^{+0.18}$ (roughly spectral type M4V). This model provides quantitative predictions for the probability any planet may have an atmosphere, which can be rigorously tested by upcoming JWST Rocky Worlds observations.

Keywords: Exoplanets (498), Planetary science (1255), Exoplanet astronomy (486), Exoplanet atmospheres (487), Planetary atmospheres (1244), Atmospheric evolution (2301), Planetary climates (2184)

1. INTRODUCTION

Where can atmospheres thrive? This question has grown more urgent as astronomers branch out from the Solar System to exoplanets, where atmospheres require great observational expense to measure or sometimes can only be imagined. A complete, precise, and predictive answer to this question might not exist, as each individual atmosphere is the integrated balance of difficult-to-model sources and sinks. Atmospheres grow through early accretion from primordial nebulae, through later impact delivery, through continual magmatic outgassing from the interior, and through evaporation or sublimation of surface volatiles. Atmospheres wither through myriad upper-atmosphere escape processes driven by stellar radiation, stellar winds, and/or impacts; through

sequestering into the interior; and through condensation or deposition to the surface. These processes continuously interact with each other, they operate on timescales spanning minutes to gigayears, and they depend on historical environmental inputs that can be wildly uncertain, chaotic, or stochastic. On Earth and other inhabited planets, atmospheric evolution is further complicated by biogeochemical cycles that may include the influence of technological civilizations. For more on atmospheric evolution, see reviews by R. E. Johnson et al. (2008); H. Lammer et al. (2008); F. Tian (2015); J. E. Owen (2019); G. Gronoff et al. (2020); R. Wordsworth & L. Kreidberg (2022) and textbooks by J. W. Chamberlain & D. M. Hunten (1987); R. T. Pierrehumbert (2010); S. Seager (2010); A. P. Ingersoll (2013); J. J. Lissauer & I. De Pater (2019).

Despite the incredible specifics needed to model an atmosphere’s detailed history, we can still seek systematic trends among basic planet properties that may al-

low for the cultivation of an atmosphere. [K. J. Zahnle & D. C. Catling \(2017, hereafter ZC17\)](#) distilled this idea into the search for a “cosmic shoreline”, with dry volatile-poor atmosphereless worlds (the sand) on one side of the shoreline and worlds rich in volatiles or atmospheres on the other (the lake/sea/ocean). ZC17 explored log-linear boundaries in 2D spaces defined by planetary escape velocity v_{esc} – a tracer of how strongly planets hold onto volatiles (or various combinations of v_{esc} with planet mass M , radius R , density ρ) – and by various sources of incoming energy available to drive escape: the current bolometric flux² planets receive f , the cumulative X-ray and extreme ultraviolet (XUV) fluence planets have received over their history $F_{\text{XUV}} = \int_0^{\text{now}} f_{\text{XUV}}(t)dt$, and/or the estimated velocity of giant impacts v_{imp} . Although it is typically less than 0.01% of a star’s bolometric luminosity ([K. France et al. 2016](#)), the difficult-to-measure XUV flux is distinctly important because it drives the upper-atmosphere heating and ionization that mediate many escape processes ([J. L. Linsky & S. Redfield 2024](#)). Stellar XUV increases dramatically on the main-sequence toward lower mass/radius/luminosity stars ([J. Linsky 2019](#); [D. J. Wilson et al. 2025](#); [E. K. Pass et al. 2025](#)). We must account for this rising XUV when comparing planets around different host stars, especially since the planets that are easiest to observe are often transiting low-mass M dwarf stars ([C. H. Blake et al. 2008](#); [P. Nutzman & D. Charbonneau 2008](#); [C. V. Morley et al. 2017](#)). ZC17 identified $f \propto v_{\text{esc}}^4$ and $F_{\text{XUV}} \propto v_{\text{esc}}^4$ as effective definitions of instellation-based cosmic shorelines, as well as $v_{\text{imp}}/v_{\text{esc}} = 5$ as a potential impact-driven shoreline (see also [K. Zahnle 1998](#)).

The ZC17 instellation-based shorelines have been adopted among the exoplanet community trying to identify rocky exoplanets most likely to have atmospheres and to contextualize non-detections of such atmospheres from JWST ([B. Park Coy et al. 2024](#); [J. Ih et al. 2025](#), and references therein). The Rocky Worlds STScI Director’s Discretionary Time program is using 500 hours of JWST time to survey terrestrial transiting exoplanets for atmospheres ([S. Redfield et al. 2024](#)) and includes estimated location relative to the F_{XUV} shoreline as a metric for target prioritization³. Since the shoreline is being used, we want to help make it as useful as possible.

² In this work we primarily use “flux” (f) to refer to the power per unit area (W/m^2) a planet receives from its star. It is equivalent to “insolation” (incoming solar radiation) as used by ZC17, “instellation” (incoming stellar radiation) introduced for exoplanets by [A. L. Shields et al. \(2013\)](#), or “irradiance.”

³ rockyworlds.stsci.edu

In this work, we revisit the ZC17’s instellation-based shorelines through the lens of Bayesian probabilistic modeling and incorporate new rocky exoplanet atmospheres constraints from JWST. We define a generative model for the probability of a planet having an atmosphere and use it to infer the location, slope, and width of a cosmic shoreline, along with uncertainties on these quantities. We expand the shoreline into 3D, using planetary escape velocity v_{esc} , planetary bolometric flux f , and stellar luminosity L_* as three predictors for whether planets have atmospheres. The inclusion of stellar luminosity is designed to remove the need for star-by-star estimates of hard-to-measure environmental drivers for atmospheric escape (like high-energy fluence F_{XUV}), moving them to where they can be modeled and marginalized more easily on an ensemble level. Thus, the predictors for atmospheres can stay rooted in easy-to-observe measurements, while still capturing trends in changing stellar environment toward lower mass stars (such as increased F_{XUV} making them more capable of eroding planetary atmospheres). Acknowledging that a true underlying cosmic shoreline is likely crinkled with fjords and peninsulas, tidepools and islands, we apply this approximate model to explore the threshold for atmospheres on both a global scale (from hot transiting exoplanets to the outer edges of the Solar System as in ZC17) and local scale (only planets where CO_2 is likely to be in the gas phase) relevant to JWST’s current detection capabilities and to habitability.

We assemble planet populations to analyze in §2, present the probability model and fitting methodology in §3, show the inferred shorelines in §4, interpret the physical implications of the derived slopes in §5, and conclude in §7. Code to reproduce all plots in the paper and calculations are linked throughout with the `</>` symbol.

2. CURATING THE DATA

We assemble planetary properties using `exoatlas` ([Z. Berta-Thompson 2025](#)), a tool for accessing, filtering, and visualizing archival planet properties. Solar System data come from JPL Solar System Dynamics tables of major planets, dwarf planets, minor planets, and moons⁴. Exoplanet data come from the NASA Exoplanet Archive’s ([J. L. Christiansen et al. 2025](#))⁵ Planetary Systems Composite Parameters table ([NASA Exoplanet Science Institute 2020a](#)) which provides as many properties as possible for each planet, but sometimes combines values from independent and possibly inconsis-

⁴ ssd.jpl.nasa.gov

⁵ exoplanetarchive.ipac.caltech.edu

tent literature sources. Where necessary, `exoatlas` can pick specific references for particular properties from the larger Planetary System table (NASA Exoplanet Science Institute 2020b), which includes every published value for every planet. Data were last retrieved on 27 February 2026 and spot-checked for outrageous planet parameter choices in the composite table for many of the key planets discussed below. In `exoatlas` all quantities have units attached with `astropy.units`, as well as uncertainties propagated through calculations with numerical samples using `astropy.uncertainty`.

2.1. What quantities do we use to predict atmospheres?

For stellar luminosity L_* , if not present in the raw table, `exoatlas` calculates it from stellar effective temperature $T_{\text{eff},*}$ and stellar radius R_* . For the average bolometric flux a planet receives $f = L_*/(4\pi a^2)$, we first attempt to pull planet semimajor axis a from the table, then, if a is not present, we attempt to calculate it from the orbital period P and stellar mass M_* via $P^2 = 4\pi^2 a^3 / GM_*$, and then finally, if necessary, from a transit-derived scaled semimajor axis ratio a/R_* . For the gravitational escape velocity of the planet v_{esc} , we calculate it as $v_{\text{esc}} = \sqrt{2GM/R}$. However, many planets have measured radii but not masses, with either radial velocity wobbles or transit-timing variations too weak to detect (transiting planets) or no moons to provide dynamical masses (small Solar System objects).

To be able to include objects without measured masses in our analysis, we derive an empirical radius-to-mass relation from rocky objects with measured masses and radii. We limit to radii smaller than $1.8R_{\oplus}$, as these are likely to be mostly terrestrial (B. J. Fulton & E. A. Petigura 2018; L. Zeng et al. 2021; J. G. Rogers et al. 2025). We fit a linear model $y = m \cdot x + b$ where we define $x_i = \ln(R_i/R_{\oplus})$ and $y_i = \ln(M_i/M_{\oplus})$, corresponding to a power-law relationship $M = CR^m$ where $C = e^b$. In addition to the measurement uncertainties on the data $\sigma_{x,i} = \sigma_{\ln R_i} = \sigma_{R_i}/R_i$ and $\sigma_{y_i} = \sigma_{\ln M_i} = \sigma_{M,i}/M_i$, we include an intrinsic scatter on the relation σ_y . We allow this intrinsic scatter to vary with radius as $\ln \sigma_y = m_{\sigma} \cdot x + b_{\sigma}$ to capture the diversity of densities that grows toward very small objects due to effects of composition, structure, and porosity. We infer the parameters of this model ($m, b, m_{\sigma}, b_{\sigma}$) following a blog post by D. Foreman-Mackey (2017, see also D. W. Hogg et al. 2010) with a Gaussian likelihood that analytically marginalizes over the uncertainties in both x and y and an uninformative prior on the slopes $P(m) \propto (1 + m^2)^{-3/2}$ as in J. VanderPlas (2014). We sample the posterior using `numpyro` (D. Phan et al. 2019) with the No U-Turns Sampler (NUTS; M. D. Hoffman & A. Gelman 2011), us-

ing 4 chains each with 5,000 warm-up steps and 50,000 samples, reaching an A. Gelman & D. B. Rubin (1992) statistic of $\hat{R} = 1.0$ and a bulk effective sample size $> 10,000$ (A. Vehtari et al. 2021, see also D. W. Hogg & D. Foreman-Mackey 2018) for all parameters. Figure 1 shows the result. The inferred slope of $m = 3.37 \pm 0.03$ is slightly steeper than a constant density ($m = 3$) as expected due to self-gravity more strongly compressing larger planets, and the intercept $b = -0.025 \pm 0.03$ is close to Earth-like ($b = 0$). The slope m is similar to but slightly lower than other mass-radius relations for rocky planets: 3.58 ($= 1/0.279$; J. Chen & D. Kipping 2017), 3.45 (J. F. Otegi et al. 2020), 3.70 ($= 1/0.27$; S. Müller et al. 2024). For the intrinsic scatter, the slope $m_{\sigma} = -0.224 \pm 0.035$ and intercept $b_{\sigma} = -1.22 \pm 0.087$ imply a 29.5% scatter at $1 R_{\oplus}$ that grows to 138% scatter at $10^{-3} R_{\oplus}$. We incorporate the sample means and covariance matrix (which describe the nearly multivariate normal posterior well) into `exoatlas` to calculate mass estimates with uncertainties that include the uncertainties on the parameters themselves, the intrinsic scatter, and the input radius uncertainties. This relation is valid only for planets without gaseous envelopes contributing significantly to their overall size.

2.2. What planets do we label as having atmospheres?

To include in our probabilistic fit we label planets (\langle / \rangle) as having an atmosphere ($A_i = 1$) or not ($A_i = 0$). Planets with inconclusive or unmeasured atmospheres remain unlabeled ($A_i = ?$) and are excluded from the fit. In both cases, to simplify the analysis, we exclude planets with quoted ages younger than 750 Myr, to minimize having to imagine the future states of still rapidly evolving planets (E. D. Lopez & J. J. Fortney 2014; H. Chen & L. A. Rogers 2016; P. C. Thao et al. 2024).

We are generous in what we call “having an atmosphere” ($A_i = 1$), as in ZC17. For Solar System bodies, we include all major planets (everything except Mercury) and moons (Titan) with atmospheric surface pressures $> 10^{-6}$ bar. We include outer Solar System moons or dwarf planets that have managed to retain significant volatile reservoirs (E. L. Schaller & M. E. Brown 2007), either as seasonally sublimating atmospheres and/or substantial global N_2 and CH_4 volatile deposits on their surfaces: Triton, Pluto, Makemake, Eris (L. A. Young et al. 2018; B. Sicardy et al. 2024; W. M. Grundy et al. 2024). We label all other Solar System objects as $A_i = 0$.

For exoplanets, planets larger than $2.2R_{\oplus}$ are extremely difficult to explain with pure rocky compositions (L. A. Rogers 2015; L. Zeng et al. 2021; J. G. Rogers et al. 2025), so we label all planets with radii

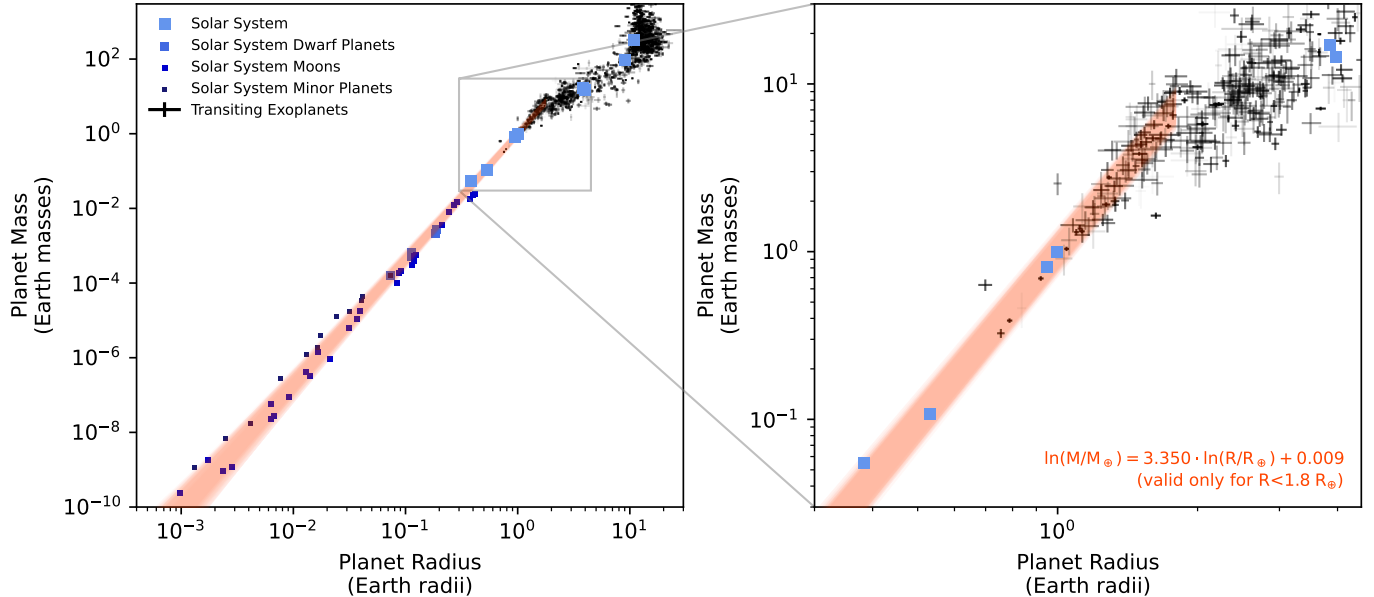


Figure 1. To determine escape velocities for objects without measured masses, we derive an empirical mass-radius relationship from exoplanets (errorbars) and Solar System objects (squares). We use this relation, valid for rocky planets up to $1.8R_{\oplus}$, to estimate planet masses and uncertainties that incorporate the intrinsic scatter on the relation, the uncertainties on the model parameters, and uncertainties on the planet radii (</>).

more than 1σ over this limit as definitely requiring atmospheres (or significant volatiles) to explain their low densities $A_i = 1$. Many planets smaller than this limit have atmospheres too, but we apply labels only to those with direct atmosphere measurements, as follows.

We apply $A_i = 1$ to two ultrahot small planets with evidence for atmospheres. 55 Cnc e shows variable JWST eclipse spectra suggesting a (potentially stochastically outgassed) CO/CO₂ atmosphere (R. Hu et al. 2024; J. A. Patel et al. 2024). TOI-561 b shows cool dayside thermal emission, suggesting a thick atmosphere to redistribute heat (J. K. Teske et al. 2025); though this cool dayside may be alternatively explained by a very reflective Bond albedo (M. Mansfield et al. 2019), the planet’s low density further strongly suggests a gaseous envelope (C. L. Brinkman et al. 2023).

We apply $A_i = 0$ to these rocky planets with eclipse observations of hot daysides that strongly suggest low albedos and poor global heat recirculation inconsistent with thick atmospheres (see D. D. B. Koll et al. 2019; M. Mansfield et al. 2019). LHS 3844b, Gl 367b, TOI-1685b have a deep eclipses, symmetric phase curves, and dark night sides (L. Kreidberg et al. 2019; M. Zhang et al. 2024; R. Luque et al. 2025). GJ 1252b, TOI-1468b, LHS 1140c, LTT 3780b, and GJ 3929b have deep photometric eclipses (I. J. M. Crossfield et al. 2022; E. A. Meier Valdés et al. 2025; M. Fortune et al. 2025; N. H. Allen et al. 2025; Q. Xue et al. 2025), and Gl 486b, GJ 1132b, and LTT 1445Ab have deep spectroscopic

eclipses (M. Weiner Mansfield et al. 2024; Q. Xue et al. 2024; P. Wachiraphan et al. 2025). TRAPPIST-1b and TRAPPIST-1c also show deep thermal eclipses (T. P. Greene et al. 2023; J. Ih et al. 2023; S. Zieba et al. 2023); although their atmosphere limits remain slightly ambiguous due to a tentative option of an inverted atmosphere on planet b (E. Ducrot et al. 2025) and systemic stellar uncertainties for both planets (W. S. Howard et al. 2023; B. V. Rackham & J. de Wit 2024; T. J. Fauchez et al. 2025; O. Lim et al. 2023; M. Radica et al. 2025; A. D. Rathcke et al. 2025), we nonetheless label them both as effectively atmosphereless. We caution that our labeling these exoplanets as $A_i = 0$ does *not* mean planets necessarily have no atmosphere at all; for tidally locked planets, a JWST measurement of hot dayside emission might only constrain the atmospheric pressure on an individual planet to less than about 1-10 bar (D. D. B. Koll 2022), really saying simply that we have not detected a very thick Venus-like atmosphere.

We leave the following notable planets unlabeled ($A_i = ?$), meaning they are ignored from the probabilistic fit, even if there have been suggestions about whether they have atmospheres. Kepler-10b and Kepler-78b have symmetric phase curves from Kepler, but with only the optical bandpass their deep eclipses are degenerate between reflected and thermal light, thus complicating atmospheric inferences (R. Sanchis-Ojeda et al. 2013; L. J. Esteves et al. 2015; R. Hu et al. 2015; V. Singh et al. 2022). K2-141 shows a K2 + Spitzer phase curve sug-

gesting a high albedo or hot inversion layer, but whether an atmosphere is absolutely required remains uncertain (V. Singh et al. 2022; S. Zieba et al. 2022). LHS 1478b and TOI-431b appear to have shallow thermal eclipses, but more data are needed to rule out systematics (P. C. August et al. 2025; C. Monaghan et al. 2025). L 98-59 b’s transmission spectrum may show tentative evidence of SO_2 (possibly from tidally-heated volcanism; D. Z. Seligman et al. 2024) but is also consistent with featureless (A. Bello-Arufe et al. 2025), so we leave it unlabeled. Otherwise, transmission spectra have not yet conclusively identified nor ruled out any rocky planet atmospheres due to degeneracies with clouds (J. Lustig-Yaeger et al. 2019) and/or stellar contamination (E. M. May et al. 2023; S. E. Moran et al. 2023); we leave all transmission spectroscopy-based non-detections as $A_i = ?$.

2.3. What do we expect atmospheres near the shoreline to be?

Though “having an atmosphere” can be partially agnostic to what makes up the atmosphere, it is worth commenting on the expected composition of planets near the shoreline. For close-in rocky planets where JWST is starting to provide atmospheric constraints, we focus on CO_2 (and to some extent O_2) as the likely major constituent of temperate atmospheres distilled by near-complete atmospheric erosion (K. Hamano et al. 2013; R. Luger & R. Barnes 2015; L. Schaefer et al. 2016; J. Krissansen-Totton et al. 2024). Venus (92 bar) and Mars (0.004 – 0.009 bar) are both about 95% CO_2 (K. Lodders & B. Fegley 1998), and Earth too would likely have about 100 bars of atmospheric CO_2 (swamping our 1 bar of $\text{N}_2 + \text{O}_2$) if not for the presence of H_2O continually raining down, dissolving atmospheric CO_2 , and locking it away into solid carbonates (J. C. G. Walker et al. 1981; C. Lécyer et al. 2000; A. P. Ingersoll 2013; R. Wordsworth & L. Kreidberg 2022; J. Hansen et al. 2025). Earth preserves its H_2O (and thus keeps our CO_2 trapped in limestone deposits) only because water precipitates before it reaches the upper atmosphere, where it would be dissociated by UV radiation and its H atoms lost to space. On warm Venus, the runaway greenhouse process (M. Komabayasi 1967; A. P. Ingersoll 1969) vaporizes water and drives it inevitably to the upper atmosphere, where its H escapes (K. Hamano et al. 2013; J. Leconte et al. 2013; R. D. Wordsworth & R. T. Pierrehumbert 2013). On cold Mars, hydrogen has also been preferentially lost (B. M. Jakosky et al. 2018), with modern escape largely driven by dust dynamics carrying frozen water up to high altitudes (M. S. Chaffin et al. 2021). CO_2 (possibly mixed with O_2) at-

mospheres are also particularly detectable for exoplanets with JWST, especially with Rocky Worlds’ use of MIRI filter photometry centered on the strong $15 \mu\text{m}$ CO_2 absorption band (C. V. Morley et al. 2017; J. Ih et al. 2023).

2.4. What limits do we consider on the cosmic shoreline?

We consider two thresholds in bolometric flux f that we suspect could potentially matter when trying to define a continuous cosmic shoreline. First, we consider a *magma ocean* boundary that we set at $f_{\text{magma}} = 1400f_{\oplus}$, corresponding to a zero-albedo global equilibrium temperature of $T_{\text{magma}} = 1700\text{K}$. Above roughly this instellation, significant surface melting may leave planets in a continuous magma ocean state (C.-É. Boukaré et al. 2022). At ultrahot temperatures, the vaporization of rock itself can generate significant atmospheres (L. Schaefer & B. Fegley 2009; L. Schaefer et al. 2012). Molten planets can also provide direct gas exchange with a much deeper mantle volatile reservoir than cooler solidified planets, potentially replenishing long-living atmospheres even in the face of strong atmospheric erosion (C. Dorn & T. Lichtenberg 2021; R. Hu et al. 2024; J. K. Teske et al. 2025). Therefore, we will exclude planets hotter than T_{magma} from our main shoreline estimate.

Second, we consider a *CO_2 freezeout* boundary at $f_{\text{freeze}} = 0.24f_{\oplus}$, corresponding to a temperature of $T_{\text{freeze}} = 194\text{K}$ (where the saturation vapor pressure of CO_2 drops below 1 bar; R. T. Pierrehumbert 2010). This f_{freeze} coincides approximately with the outer edge of the habitable zone, defined where CO_2 can no longer provide greenhouse warming because it condenses out of the atmosphere (R. K. Kopparapu et al. 2013). While worlds cooler than T_{freeze} can obviously still have atmospheres, the sources and sinks for those atmospheres (mostly H_2 , CH_4 , N_2 in the Solar System) may differ from temperate terrestrial planets’ CO_2 -dominated atmospheres. We will include planets cooler than T_{freeze} in our main shoreline estimate, but we will also test the effect of restricting to only planets warm enough for CO_2 to remain gaseous.

With these two thresholds, we define three samples of planets. We will compare the shorelines inferred from each sample below.

- *No magma ocean*: Our main analysis includes all planets $f < f_{\text{magma}}$, comprising 869 $A_i = 1$ and 48 $A_i = 0$ worlds. This sample includes the entire Solar System and all but a few of the hottest exoplanets.
- *No magma ocean, no CO_2 freezeout*: As an auxiliary test, we consider only planets between

$f_{\text{freeze}} < f < f_{\text{magma}}$, including 858 $A_i = 1$ and 17 $A_i = 0$. This sample excludes the outer Solar System, effectively examining the shoreline for non-molten planets out to Mars-like orbits.

- *Any temperature:* As another auxiliary test, we include all objects, with no limits on f , with 1026 $A_i = 1$ and 48 $A_i = 0$. This sample includes the ultrahot planets TOI-561 b and 55 Cnc e, which are above the f_{magma} flux limit.

3. FITTING A COSMIC SHORELINE

We construct a generative model that tries to explain the atmosphere labels A_i for planet i using the predictors

$$\log_{10} \left(\frac{f_{\text{shoreline}}}{f_{\oplus}} \right) = \log_{10} \left(\frac{f_0}{f_{\oplus}} \right) + p \cdot \log_{10} \left(\frac{v_{\text{esc}}}{v_{\text{esc},\oplus}} \right) + q \cdot \log_{10} \left(\frac{L_{\star}}{L_{\odot}} \right). \quad (2)$$

f_i , $v_{\text{esc},i}$, $L_{\star,i}$. We first define a cosmic shoreline flux $f_{\text{shoreline}}$ for escape velocity v_{esc} and stellar luminosity L_{\star} with the power law expression

$$f_{\text{shoreline}} = f_0 \left(\frac{v_{\text{esc}}}{v_{\text{esc},\oplus}} \right)^p \left(\frac{L_{\star}}{L_{\odot}} \right)^q \quad (1)$$

where f_0 , p , and q are model parameters, $v_{\text{esc},\oplus} = 11.18$ km/s is Earth's escape velocity, and $L_{\odot} = 3.828 \times 10^{26}$ W is the Sun's luminosity. We compare all fluxes to Earth's average bolometric flux $f_{\oplus} = L_{\odot}/(4\pi a)^2 = 1361 \text{ W/m}^2$. This power law log transforms to a linear plane in 3D space

We define a distance from this shoreline in log-flux as

$$\Delta = \log_{10} \left(\frac{f}{f_{\oplus}} \right) - \log_{10} \left(\frac{f_{\text{shoreline}}}{f_{\oplus}} \right) = \log_{10} \left(\frac{f}{f_{\text{shoreline}}} \right) \quad (3)$$

which is similar to the Atmosphere Retention Metric from E. K. Pass et al. (2025) and P. Meni-Gallardo & E. Pallé (2025). We use this distance to describe the probability of each planet having an atmosphere with the logistic function (see Ž. Ivezić et al. 2020) as

$$p_i = P(A_i = 1 | \mathbf{x}_i, \boldsymbol{\theta}) = \frac{1}{1 + e^{\Delta_i/w}} \quad (4)$$

where the predictors for each datum are $\mathbf{x}_i = [\log_{10}(f_i/f_{\oplus}), \log_{10}(v_{\text{esc},i}/v_{\text{esc},\oplus}), \log_{10}(L_{\star,i}/L_{\odot})]$ and the model parameters are $\boldsymbol{\theta} = [f_0, p, q, w]$. This logistic function smoothly transitions from 1 when f is below the shoreline to 0 above, with the width parameter w describing the fuzziness of the shoreline, how quickly in $\log_{10}(f/f_{\oplus})$ planets change from mostly having atmospheres to mostly not. The likelihood of the data ensemble \mathbf{A} can be calculated by multiplying $p_i^{A_i}$ (= how well did we predict the presence of an atmosphere) by $(1 - p_i)^{1 - A_i}$ (= how well did we predict the absence of an atmosphere) across all data points (a Bernoulli distribution):

$$P(\mathbf{A} | \boldsymbol{\theta}) = \prod_{i=1}^N p_i^{A_i} \cdot (1 - p_i)^{1 - A_i} \quad (5)$$

This likelihood $P(\mathbf{A} | \boldsymbol{\theta})$ and a prior $P(\boldsymbol{\theta})$ together determine the posterior probability $P(\boldsymbol{\theta} | \mathbf{A}) = P(\mathbf{A} | \boldsymbol{\theta})P(\boldsymbol{\theta})$.

For f_0 , we adopt an uninformative uniform prior on $\log_{10}(f_0/f_{\oplus})$. For p , and q , we adopt the uninformative prior $P(\boldsymbol{\theta}) \propto (1 + p^2)^{-3/2} \cdot (1 + q^2)^{-3/2}$, which avoids the infinitely growing prior space toward high slope values and effectively represents a uniform prior on the rotation angle of the slopes in log space (see J. VanderPlas 2014). For w , we adopt a uniform prior of $-6 > \ln w > 2$, spanning $0.0024 \text{ dex} < w < 7.4 \text{ dex}$, or from a 0.57% change in f at the narrowest to a factor of 2.5×10^7 change in f at the widest; practically we find that allowing narrower widths than this can reveal sharp discontinuities that become difficult to sample.

To account for measurement uncertainties on the predictors, the expression for p_i in Equation 4 should be marginalized over the distribution of true (unknown) values for each planet's \mathbf{x}_i . While this marginalization can sometimes be done analytically (as in the mass-radius fit in §1), we were unable to find a simple analytic expression and instead relied on the remarkable efficiency of `numpyro`'s NUTS sampler to do this marginalization numerically. We introduced three parameters for each datapoint (up to 1,074 planets or 3,222 parameters) to represent the true values of \mathbf{x}_i , with normal priors centered on the measured values and the uncer-

tainties as their widths, and we sampled these alongside the 4 parameters θ we actually care about.

We used `numpyro` with NUTS to sample from this posterior, running 4 chains with 5,000 warm-up steps and 50,000 samples each, always achieving a Gelman-Rubin statistic of 1.0 across the chains and usually achieving an effective sample size always (and sometimes much) larger than 1,000 ($\langle \nu \rangle$). Even with the thousands of hyperparameters we use to marginalize over measurement uncertainties, this sampling takes only a few minutes on a modern MacBook Pro. We repeat these fits, with and without uncertainties, across various subsamples of the data ($\langle \nu \rangle$).

4. SHORELINES IN 3D

Below, we present this newly inferred shoreline model and explore the meaning of its parameters in §4.1. We present additional tests that probe the sensitivity of this shoreline to changing planet samples or modeling assumptions in §4.2, §4.3, §4.4.

4.1. A New Cosmic Shoreline

Figures 2 and 3 show the inferred shoreline model. All Solar System worlds and exoplanets in the “no magma ocean” sample were used to determine the shoreline parameters. Although not included in the fit, the ultrahot magma-ocean planets are still shown for context. Because the probability of an atmosphere A is a function in a 3D volume, it can be a little tricky to visualize in a single plot. In Figure 2 we display this 3D volume in slices: each row holds one dimension fixed to a narrow range and visualizes the other two dimensions on the x and y axes, and each column displays a different range of values for the fixed dimension. The background color shows the modeled probability of an atmosphere at each (x, y) location in each slice, marginalized (= integrated, see D. W. Hogg et al. 2010; D. S. Sivia & J. Skilling 2011; J. VanderPlas 2014; Ž. Ivezić et al. 2020) over both the width of the slice and the uncertainties on the model parameters. Even for infinitely thin slices with no parameter uncertainties the transition would still appear fuzzy due to the intrinsic width w (see Equation 4). Figure 3 shows an animated version, stepping through slices in stellar luminosity.

The top row (a-d) of Figure 2 holds L_\star as the fixed dimension, decreasing from solar type host stars on the left to the latest possible M dwarf stars on the right. The centers of these luminosity ranges ($1L_\odot$, $0.1L_\odot$, $0.01L_\odot$, $0.001L_\odot$) correspond to main-sequence spectral types (G2, K7, M3.5, and M6) according to the M. J. Pecaut & E. E. Mamajek (2013) sequence. Panel (a) shows v_{esc} and bolometric flux f for both Solar System

objects (all with $L = 1.0L_\odot$) and exoplanets with host stars within a factor of $\sqrt{10}$ of the Sun’s luminosity; it is the closest analog to Figure 1 from ZC17, which shows similar quantities but without the restriction on exoplanet host star type. The shoreline in this row has a slope of p (see Equation 2) and reading from left to right appears to recede (to borrow the visual metaphor from E. K. Pass et al. 2025) down and to the right, with the bolometric threshold $f_{\text{shoreline}}$ decreasing at fixed v_{esc} toward lower luminosity stars.

The middle row (e-h) shows shoreline slices for different fixed v_{esc} , increasing from tiny low-mass dwarf planets on the left to gas giants on the right. Only Solar System objects are known at low v_{esc} (e), but for Earth-like v_{esc} values (g) exoplanet atmosphere data become available either as radii large enough to require volatiles or as rocky planets with JWST hot dayside brightness temperatures disfavoring thick atmospheres. In these slices the visible slope is $1/q$, with cooler less luminous stars having lower maximum allowable flux levels $f_{\text{shoreline}}$ for atmospheres to survive.

The bottom row (i-l) shows the shoreline for different fixed f , increasing from the cold outer regions of the Solar System on the left to the very hottest exoplanets on the right. The slope of the shoreline in this projection is $-q/p$ and indicates a larger v_{esc} is necessary in order for lower L_\star hosts to permit atmospheres. For temperate planets (j), if we imagine shrinking the host star luminosity while keeping f constant at f_\oplus , Mars-sized planets would be unable to retain atmospheres around stars less luminous than $0.1 L_\odot$, and Earth/Venus-size planets would likely lose atmospheres somewhere between $10^{-3} - 10^{-2} L_\odot$.

Figure 4 shows the posterior probability distributions for the shoreline parameters. We show both the main fit including all planets together and what we might learn from just Solar System or just exoplanets each by themselves. We compare these posteriors with `corner.py` (D. Foreman-Mackey 2016), with contours in each 2D panel that enclose 68.3% and 95.4% of the probability marginalized over other parameters.

We find the intercept to be $\log_{10} f_0 = 2.62^{+0.45}_{-0.31}$, meaning that an Earth-size planet orbiting a Sun-like star should on average be able to retain an atmosphere with bolometric flux levels f/f_\oplus up to about $10^{2.62} = 414$. If we moved Earth inward toward the Sun, hydrogen and the hope of habitability would be lost long before this limit, likely leaving heavily oxidized CO_2/O_2 atmospheres. Yet, these dense atmospheres apparently might be retained even up to surprisingly high temperatures.

The escape velocity slope $p = 5.9^{+0.61}_{-0.43}$ is steeper than $p = 4$ chosen by ZC17 and means that a factor of $10 \times$

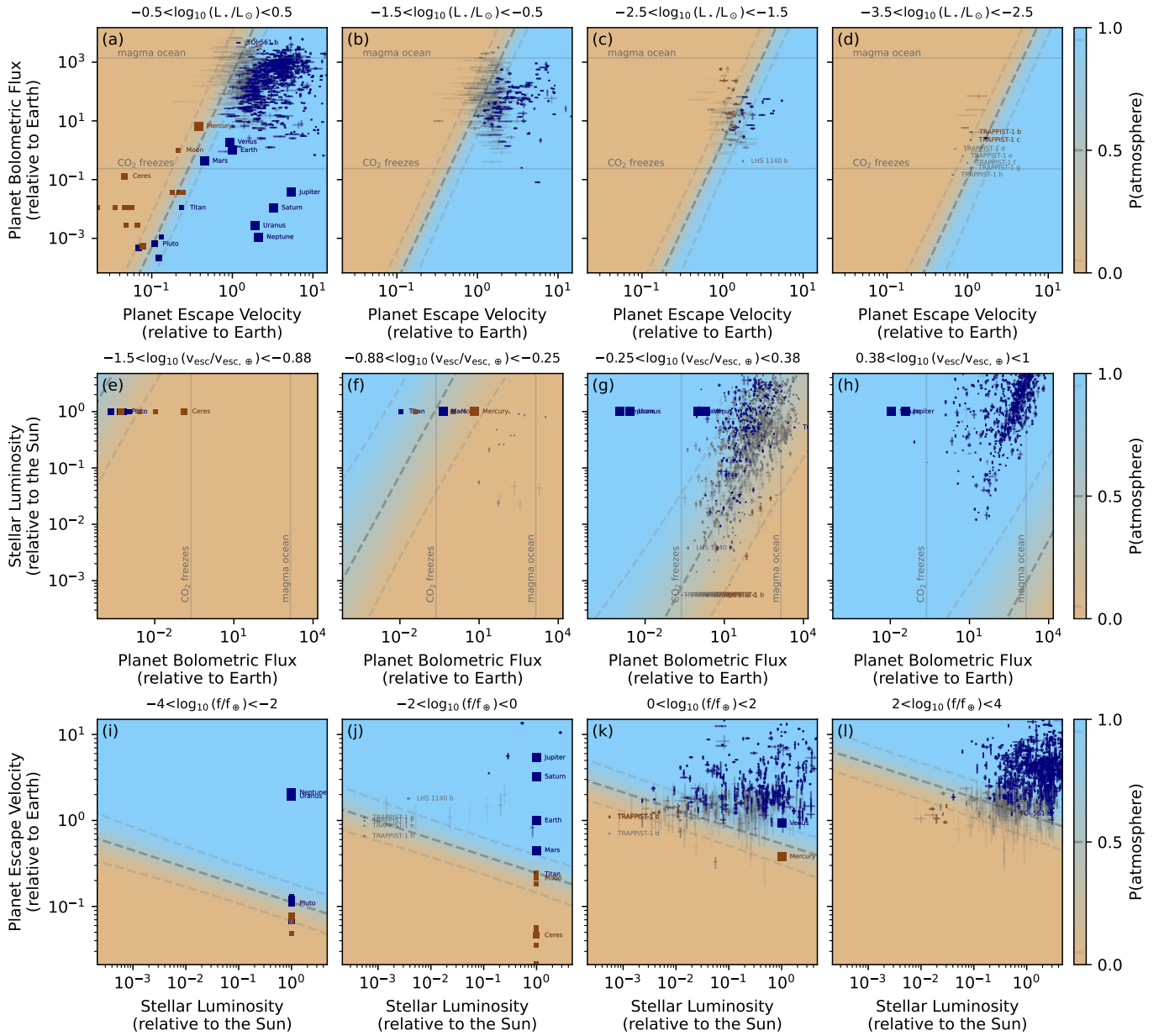


Figure 2. A cosmic shoreline dividing exoplanets (errorbars) and Solar System planets (squares) with any type of atmosphere or global surface volatiles (blue symbols, $A_i = 1$) from those without (brown symbols, $A_i = 0$). Magma ocean planets ($T_{\text{eq}} > 1700\text{K}$) were excluded from the fit but are still shown for context, as are planets without definitive atmosphere constraints (gray symbols, $A_i = ?$). The shoreline defines a plane in the 3D space of (f, v_{esc}, L) ; each row shows slices that consider a narrow range of stellar luminosity (top), planet escape velocity (middle), and planet flux (bottom). Background colors indicate the modeled probability of an atmosphere at each location (sandy brown for $p_i = 0$, water blue for $p_i = 1$), marginalizing over the parameter uncertainties and the width of the slice; contours (dashed lines) highlight atmosphere probabilities of 5%, 50%, 95% ($</>$).

increase in v_{esc} causes the critical flux $f_{\text{shoreline}}$ to move up by about $10^{5.9}$. Notably, for Solar System planets alone we find $p = 3.76^{+0.73}_{-0.51}$ and for exoplanets alone we find $p = 6.37^{+3.1}_{-2.2}$. Each is individually consistent with $p = 4$, so the higher joint slope reflects a compromise where these two different samples that mostly occupy different regions of parameter space can agree (see Figure 4).

The stellar luminosity slope $q = 1.17^{+0.28}_{-0.20}$ means that if we decrease the luminosity of the host star by $10\times$, the maximum flux that permits atmospheres $f_{\text{shoreline}}$ decreases by a factor $10^{1.17}$. This is steep! If we take $f_{\text{hz}} = f_{\oplus}$ as a crude approximation for the habitable zone (neglecting the important dependence on the stellar spectrum; R. K. Kopparapu et al. 2013), this fit implies $f_{\text{shoreline}} < f_{\text{hz}}$ for stars less luminous than

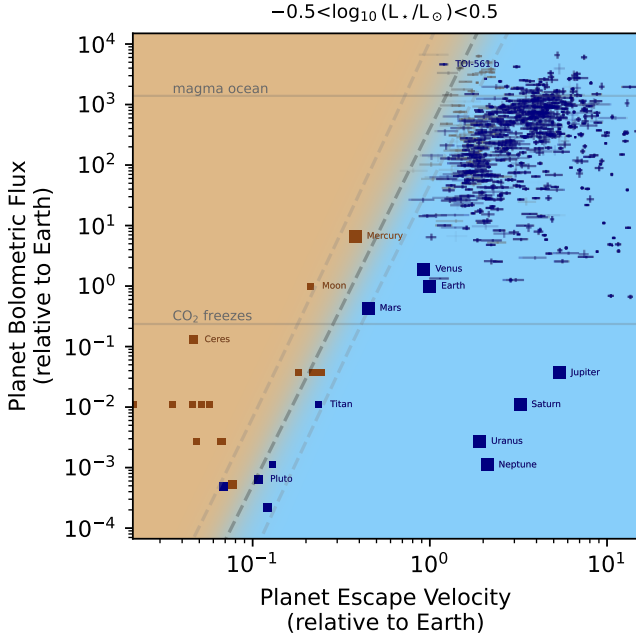


Figure 3. The same cosmic shoreline as the top row of Figure 2, but expressed as an animation that is available in the HTML version of the article, showing the 3D shape of the cosmic shoreline by stepping through slices of changing stellar luminosity (</>).

$\log_{10}(L_*/L_\odot) = -2.23^{+0.18}_{-0.21}$ or $L_*/L_\odot = 0.006^{+0.003}_{-0.002}$, corresponding to M4V spectral type (M. J. Pecaut & E. E. Mamajek 2013) or $0.25M_\odot$ mass (J. S. Pineda et al. 2021a). We further discuss the steep q slope’s implications for habitability in §6.3.

The intrinsic width of the shoreline $\ln w = -1.40^{+0.32}_{-0.30}$, or $w = 0.247^{+0.092}_{-0.065}$ dex, means that if f increases by a factor of $10^{0.247}$ above $f_{\text{shoreline}}$ then the probability of an atmosphere drops from 50% to $1/(1 + e^1) = 27\%$ (Equation 4). To translate into more familiar probabilities from a normal distribution, the chance of having an atmosphere drops to 32% (100% - 68%, which might colloquially be called a 1σ upper limit) and 5% (2σ upper limit) at $0.75w$ and $2.94w$, respectively. We define w_{95} as the width of the transition from atmospheres being 95% likely to only 5% likely, which corresponds to $w_{95} = 5.89w = 1.46^{+0.54}_{-0.38}$ dex or a factor of $28.7^{+71}_{-17}\times$ in flux (</>). The blending of colors and the dashed 5 – 95% lines in Figures 2 and 3 include the fuzziness from this w , along with marginalization over the uncertain shoreline parameters and the finite width of the visualization slice.

4.2. Sensitivity to planet flux limits.

Our main shoreline fit uses planets from the “no magma ocean” sample (§2.4), excluding planets that re-

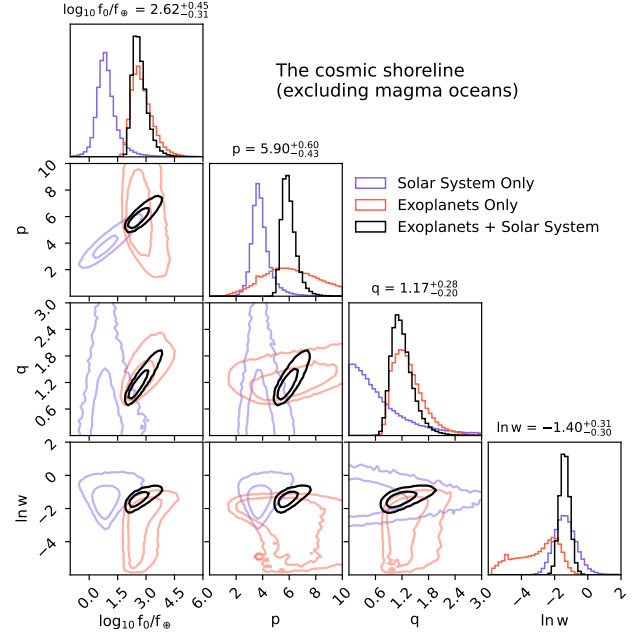


Figure 4. Cosmic shoreline parameter posterior probabilities, including only planets cool enough to avoid global magma oceans. These parameters define the atmosphere probability shown in Figure 2. Panels show marginalized 1D histograms (diagonal) and marginalized 2D distributions (off-diagonal) with contours that enclose 68.3% and 95.4% probability. Titles along the diagonal show central 68.3% confidence intervals for the exoplanets + Solar System joint fit. The model parameters define a shoreline via $\log_{10}(f_{\text{shoreline}}/f_\oplus) = \log_{10}(f_0/f_\oplus) + p \log_{10}(v_{\text{esc}}/v_{\text{esc},\oplus}) + q \log_{10}(L_*/L_\odot)$, with w representing the logistic width parameter setting the fuzziness of the shoreline (</>).

ceive fluxes above the magma ocean flux limit f_{magma} to avoid the larger volatile inventories accessible in these planets’ atmospheres. Here, we briefly explore the effect of applying different flux limits to the sample of planets we consider.

If we zoom in, also excluding planets with fluxes below the CO_2 freeze-out flux limit f_{freeze} (“no magma ocean, no CO_2 freezeout”), we find the shoreline fit shown in Figure 5. The advantage of removing the colder worlds is that we can more confidently compare broadly similar atmospheres, where planetary climates are fundamentally set by the planets’ resilience for retaining gaseous CO_2 . Much colder CH_4 and N_2 atmospheres or surface volatile reservoirs like Titan’s or Pluto’s may represent fundamentally different formation and evolution pathways, and might therefore exhibit different shorelines. The disadvantage of excluding cool planets is that we remove the entire outer Solar System, which provides considerable leverage on the shoreline slopes (particularly p). The inferred slopes $p = 6.3^{+1.7}_{-1.3}$ and $q = 1.27^{+0.37}_{-0.25}$ (Figure 6) indeed do have larger uncertainties than for

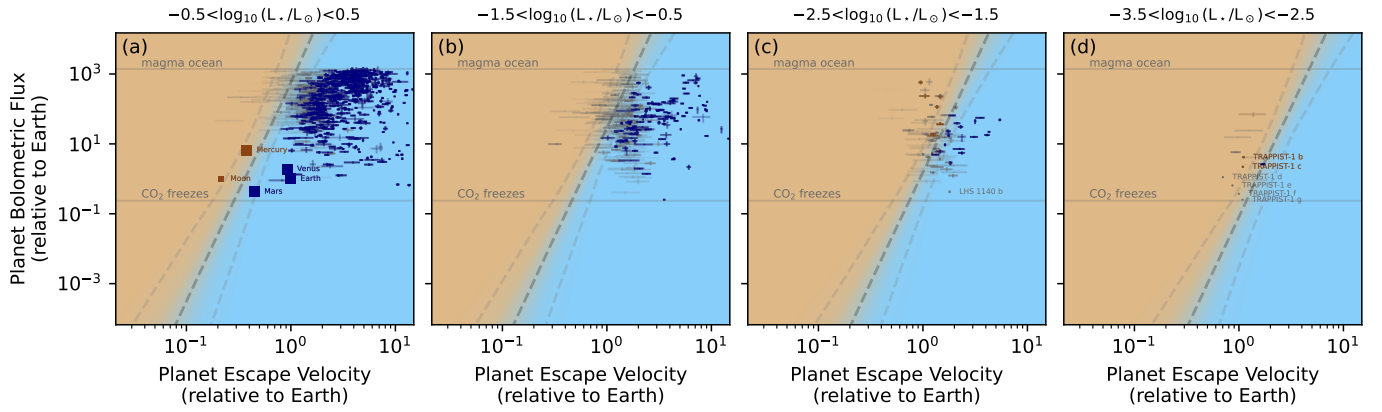


Figure 5. A cosmic shoreline exactly as in the top row of Figure 2, but specifically targeting CO₂-dominated atmospheres in the “no magma ocean, no CO₂ freezeout” sample with equilibrium temperatures warm enough for CO₂ to exist as a gas ($T_{\text{CO}_2} > 194\text{K}$) and cool enough that a global magma ocean is less likely ($T_{\text{magma}} < 1700\text{K}$). This more narrowly defined cosmic shoreline matters because CO₂ is both likely in warm secondary atmospheres and relatively easier to detect for exoplanets in thermal emission with JWST (</>).

the main sample. Yet, the slopes are consistent between the two samples.

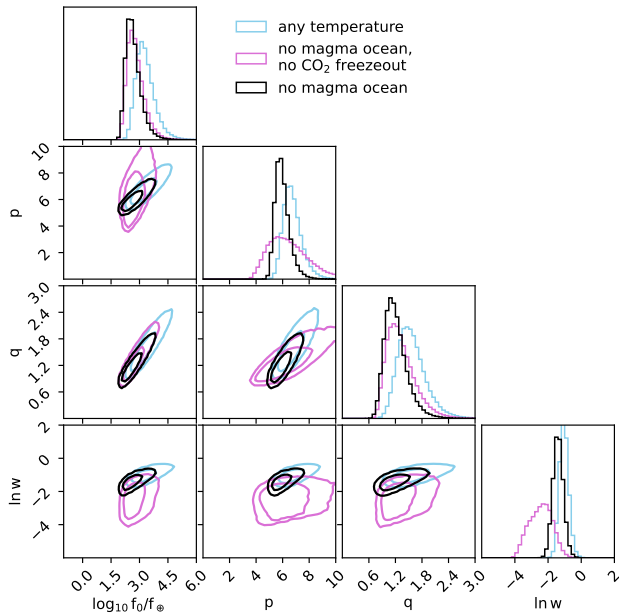


Figure 6. Cosmic shoreline parameter posterior probabilities considering planets that fall within three different bolometric flux limits, using exoplanet and Solar System data in all fits. Panels show marginalized 1D histograms (diagonal) and marginalized 2D distributions (off-diagonal) with contours that enclose 68.3% and 95.4% probability. The model parameters define a shoreline via $\log_{10}(f_{\text{shoreline}}/f_{\oplus}) = \log_{10}(f_0/f_{\oplus}) + p \log_{10}(v_{\text{esc}}/v_{\text{esc},\oplus}) + q \log_{10}(L_*/L_{\odot})$, with w representing the logistic width parameter setting the fuzziness of the shoreline (</>).

If we zoom out, excluding no planets, even those hot enough for continuously molten surfaces (“any temper-

ature”), the shoreline shifts. One planet, TOI-561 b (J. K. Teske et al. 2025, shown in Figure 2a), nudges the shoreline toward steeper slopes $p = 6.67^{+0.77}_{-0.58}$ and $q = 1.54^{+0.35}_{-0.27}$ (Figure 6) to try to capture the apparent atmosphere on this ultrahot world transiting a roughly Sun-like star. That TOI-561b prefers a different shoreline than the “no magma ocean” sample marginally confirms the hypothesis that lava worlds may have access to deeper pools atmospheric volatiles and that their abilities to support atmospheres cannot be simply extrapolated to more temperate planets.

Curiously, the width of the shoreline shows a tentative trend of decreasing w toward tighter population flux limits (Figure 6) with $\ln w = -1.05^{+0.28}_{-0.26}$ for “any temperature”, $\ln w = -1.40^{+0.32}_{-0.30}$ for “no magma ocean”, $\ln w = -2.41^{+0.67}_{-0.76}$ for “no magma ocean, no CO₂ freezeout”. One possibility is that the width w on broad global scales is partially capturing unknown curvature or topography along the shoreline. A lower w in the zoomed-in sample might hint at the log-linear shoreline being a better local description on increasingly fine scales. More thoroughly testing for such local geography to the shape of the shoreline will require many more planets with reliable atmosphere labels.

4.3. Sensitivity to Including Gas Giant Planets

In the above fits, we did not place upper limits on planet escape velocity or radius, allowing all giant planets to participate in sculpting the shoreline, as in ZC17. Hot Jupiters could potentially bias the shoreline slope, in that they might lose tens of Earth masses of atmosphere but still appear as $A_i = 1$. We tested the sensitivity of the inferred shoreline to this concern by repeating the fits including only planets smaller than Neptune. We found no significant changes to the parameters, likely

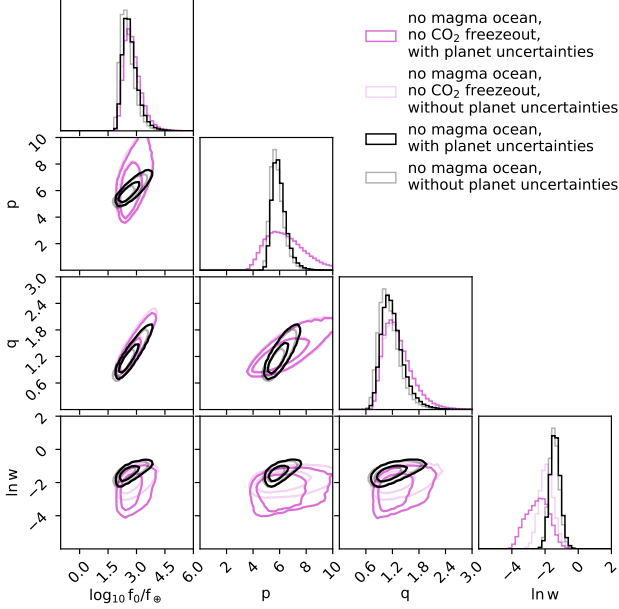


Figure 7. Posteriors inferred with (intense lines) and without (faint lines) accounting for uncertainties on planet properties (f , v_{esc} , L_{\star}). Two planet flux limits are shown, using exoplanet and Solar System data in all fits. Marginalizing over uncertainties barely matters for the large “no magma ocean” sample but broadens the possible intrinsic shoreline widths w for the smaller “no magma ocean, no CO_2 freeze-out” sample to lower values, because w is less necessary when planets’ scatter can be explained by their own measurement uncertainties ($\langle \! / \! \rangle$).

because hot Jupiters all have such high surface gravities that they fall well within the volume where atmospheres are inevitably strongly predicted.

4.4. Sensitivity to Planet Parameter Uncertainties

We test the impact that measurement uncertainties on the predictors v_{esc} , f , L_{\star} have the inferred shoreline. Figure 7 shows parameter posteriors with and without including parameter uncertainties for two of the planet subsamples. Including planet uncertainties slightly broadens distributions and also allows for lower values of w , where disagreeing labels at fixed shoreline distance Δ ; can be a little more explained by uncertainties on the predictors and thus requiring less intrinsic fuzziness. This is especially true for the smallest “no magma ocean, no CO_2 freezeout” sample; with fewer planets, the uncertainty on each planet’s position relative to the shoreline matters more. Still, the differences are minor for all fits, likely because parameter uncertainties for most well-characterized planets are smaller than the fuzziness already being captured in the intrinsic width w .

5. PHYSICAL INTERPRETATION

Atmospheric loss is fundamentally a matter of energy balance: whatever energy a planet receives from its star (or still-cooling interior; see A. Gupta & H. E. Schlichting 2019), must either radiate away or be carried away in the gravitational potential energy of escaping gas (J. S. Lewis & R. G. Prinn 1984; J. W. Chamberlain & D. M. Hunten 1987). The incoming energy need not be radiative, with particles and fields in the stellar wind also driving loss, and moreso during coronal mass ejections (H. Lammer et al. 2007; B. M. Jakosky et al. 2015). Modeling efforts beyond ZC17 have included various atmospheric sources and sinks to understand where atmospheres can or cannot flourish (F. Tian 2009; R. Luger et al. 2015; J. E. Owen & Y. Wu 2017; M. C. Wyatt et al. 2020; A. Gupta & H. E. Schlichting 2021; R. D. Chatterjee & R. T. Pierrehumbert 2024; L. Chin et al. 2024; M. T. Gialluca et al. 2024; K. E. Teixeira et al. 2024; L. Zeng & S. B. Jacobsen 2024; G. Van Looveren et al. 2024, 2025; E. J. Lee & J. E. Owen 2025; X. Ji et al. 2025). Here, we briefly try to contextualize the newly inferred shoreline parameters through the lens of hydrodynamic escape, as the most efficient path for atmospheric erosion in extreme environments where XUV heating can overwhelm infrared cooling in the tenuous upper atmosphere and drive fluid flows (M. Sekiya et al. 1980; A. J. Watson et al. 1981).

For the flux slope p , we can consider a simplified model of energy-limited escape, where some fraction ϵ_{esc} of incoming power from f_{XUV} radiation converts directly into gravitational potential energy of outflowing atmosphere (A. J. Watson et al. 1981), can be written as $\epsilon_{\text{esc}} f_{\text{XUV}} \pi R_{\text{XUV}}^2 \approx GM \dot{M}_{\text{atm}} / R_{\text{atm}}$ with πR_{XUV}^2 as the planet’s cross-section to high-energy radiation, \dot{M}_{atm} as the atmospheric mass loss rate, and R_{atm} as the effective radius from which atmosphere is escaping. If we neglect important radiative and tidal effects (see H. Lammer et al. 2003; N. V. Erkaev et al. 2007), crudely approximate $R_{\text{XUV}} \approx R_{\text{atm}} \approx R$, parameterize the high-energy flux as some fraction of the bolometric flux $f_{\text{XUV}} = \epsilon_{\text{XUV}} f$, imagine the atmospheric volatile budget eroded over the system age t to be some fraction of planet mass $\dot{M}_{\text{atm}} = \epsilon_{\text{atm}} M / t$, and define $\epsilon_{\text{?}} = \epsilon_{\text{atm}} \cdot \epsilon_{\text{esc}}^{-1} \cdot \epsilon_{\text{XUV}}^{-1}$ as a *deeply* uncertain combined efficiency factor, we would find a shoreline that scales with bolometric flux as $f \propto \epsilon_{\text{?}} M^2 / R^3 \propto \epsilon_{\text{?}} v_{\text{esc}}^4 / R \propto \epsilon_{\text{?}} v_{\text{esc}}^3 \sqrt{\rho}$ as in Figure 3 of ZC17. If we use the mass-radius relation in Figure 1 to estimate $R \propto v_{\text{esc}}^{0.843 \pm 0.011}$ or $M \propto v_{\text{esc}}^{2.84 \pm 0.011}$ for rocky planets, we find $f \propto \epsilon_{\text{?}} v_{\text{esc}}^p$ with $p \approx 3.16$. Strong dependencies lurk inside $\epsilon_{\text{?}}$ that could tilt the flux slope p away from this cartoon $p = 3.16$ value, either globally or locally: ϵ_{atm} depends on volatile delivery

history, interior-atmosphere exchange, instellation, and tides (L. T. Elkins-Tanton & S. Seager 2008; L. Schaefer et al. 2016; E. S. Kite et al. 2016; D. Z. Seligman et al. 2024), and ϵ_{esc} depends (at least) on instellation, planet mass, and composition (R. A. Murray-Clay et al. 2009; J. E. Owen & A. P. Jackson 2012; J. E. Owen & Y. Wu 2017; R. D. Chatterjee & R. T. Pierrehumbert 2024; X. Ji et al. 2025; E. J. Lee & J. E. Owen 2025).

Another useful reference slope p comes from a common threshold for mass loss: the escape parameter $\lambda = v_{\text{esc}}^2/v_{\text{thermal}}^2$, where $v_{\text{thermal}} = \sqrt{2k_{\text{B}}T/m}$ is the thermal speed of the gas, with k_{B} as the Boltzmann constant, T as temperature, and m as the mass each escaping atom/molecule (see E. L. Schaller & M. E. Brown 2007; R. E. Johnson et al. 2008; G. Gronoff et al. 2020). If we calculate this escape parameter λ with planets’ zero-albedo instantaneous equilibrium temperature $T = T_{\text{eq}} \propto f^{1/4}$ (horribly inaccurately for thick atmospheres because it ignores XUV heating, but effectively setting a lower limit on atmospheric temperatures), constant values λ would correspond to $v_{\text{esc}}^2 \propto f^{1/4}$ and a shoreline slope $p = 8$. One reason the slope in energy-limited escape is shallower than this is because XUV-heated exospheres converge through infrared cooling thermostats to similar hot temperatures despite strongly varying incoming fluxes (J. W. Chamberlain 1962; R. A. Murray-Clay et al. 2009; R. D. Chatterjee & R. T. Pierrehumbert 2024). That our inferred slope $p = 5.9_{-0.43}^{+0.61}$ falls between the cartoon energy-limited and constant escape parameter limits is encouraging, but gleaning reliable insights into atmospheric evolution requires more detailed predictive modeling of the flux slope p .

For the stellar luminosity slope q , we might interpret it as setting the fraction of light a star emits in the XUV via $\epsilon_{\text{XUV}} = L_{\text{XUV}}/L_{\star} = \epsilon_{\text{XUV},\odot}(L_{\star}/L_{\odot})^{-q}$ where $\epsilon_{\text{XUV},\odot}$ is the solar XUV fraction (2×10^{-6} for the quiet Sun and higher when integrated over its lifetime T. N. Woods et al. 2009; K. France et al. 2016). Positive shoreline slopes $q > 0$ correspond to fainter stars emitting fractionally more of their luminosity in the XUV (as they do; D. J. Wilson et al. 2025), thus requiring the threshold bolometric flux $f_{\text{shoreline}}$ to decrease to keep F_{XUV} fixed. A single power law is clearly only an approximation to a more complicated picture: stars’ XUV spectra are messy functions of age (I. Ribas et al. 2005; N. J. Wright et al. 2011; J. S. Pineda et al. 2021b; G. M. Duvvuri et al. 2023; G. W. King et al. 2025), stellar type (J. L. Linsky et al. 2014; T. Richey-Yowell et al. 2019; S. Peacock et al. 2020; D. J. Wilson et al. 2025), rotational history (J. Irwin et al. 2007; R. O. P. Loyd et al. 2021; C. P. Johnstone et al. 2021), and flaring activity (K. France et al. 2020; H. Diamond-Lowe et al.

2021; A. D. Feinstein et al. 2022). ZC17 integrated old scaling relations to estimate an F_{XUV} scaling that translates to $q_{\text{ZC17}} = 0.6$ (their Equation 26). E. K. Pass et al. (2025) updated this integral with modern M dwarf data, provided F_{XUV} in mass bins spanning $0.1 - 0.3M_{\odot}$ ($-3.1 < \log_{10} L_{\odot} < -2.0$; their Table 1), and found the ZC17 expression under-predicted historic F_{XUV} fluences by $2 - 3 \times$ for these mid-to-late M dwarfs. The E. K. Pass et al. (2025) estimates do not follow a constant $d \ln \epsilon_{\text{XUV}}/d \ln L_{\star}$ across the mass range but are bounded by scalings of $q_{P25} = 0.79_{-0.11}^{+0.04}$ (median and full range, for different mass bins) relative to the Sun (\langle / \rangle). Our inferred $q = 1.17_{-0.20}^{+0.28}$ is higher than these estimates, suggesting an even stronger trend toward M dwarfs being inhospitable to planetary atmospheres.

G. Van Looveren et al. (2025) modeled escape across stellar type including realistic stellar/rotational/activity evolution and self-consistent XUV-heated thermospheres (C. P. Johnstone et al. 2018), finding thermal escape from stars’ most active periods was sufficient to erode CO_2/N_2 atmospheres out to the habitable zone for all stars less massive than about $0.4M_{\odot}$ ($\log_{10}(L_{\star}/L_{\odot}) = -1.7$, see J. S. Pineda et al. 2021a). We can translate this statement about atmospheric retention in the habitable zone via $q = -[\log_{10}(f_0/f_{\text{shoreline}}) + p \log_{10}(v_{\text{esc}}/v_{\text{esc},\oplus})] / \log_{10}(L_{\star}/L_{\odot})$ with $f_{\text{shoreline}} = f_{\text{hz}} = f_{\oplus}$ and $v_{\text{esc}}/v_{\text{esc},\oplus} = 1$, finding $q_{VL25} = 1.54_{-0.18}^{+0.27}$. That our inferred slope of $q = 1.17_{-0.20}^{+0.28}$ is consistent with this theoretical prediction suggests interpreting q as primarily representing a rough XUV scaling might be reasonable. In the future, more detailed modeling of how drivers of atmospheric loss scale with stellar luminosity, including both XUV and other non-thermal drivers like stellar wind properties, could improve on the simple power law with slope q assumed here.

6. IMPLICATIONS

Here, we place this new inferred shoreline in context. We compare to ZC17 in §6.1, predict atmosphere probabilities for planned Rocky Worlds targets in §6.2, and consider the overlap between the cosmic shoreline and the habitable zone in §6.3.

6.1. Comparison to ZC17

How does this updated shoreline model compare to the original ZC17 formulation? Figure 8 shows how this new shoreline compares to the traditional estimate of the XUV-driven cosmic shoreline (Figure 2 of K. J. Zahnle & D. C. Catling 2017). We neglect parameter uncertainties on $\log_{10}(f_0/f_{\oplus})$, p , q , $\ln w$. We collapse all stellar luminosities onto one plot, using color to indicate L_{\star}

for individual planets and the appropriate L_* -dependent shoreline to which they should be compared. The slope $p = 5.9^{+0.61}_{-0.43}$ is steeper than ZC17's $p = 4$. The dependence on stellar luminosity $q = 1.17^{+0.28}_{-0.20}$ is also stronger than the effective $q = 0.6$ underlying ZC17's estimate of planets' cumulative XUV history (see §5), as seen by the wider spacing between lines of different L_* . Relative to ZC17, the new inferred shoreline is more generous to hot planets around hot stars, but similarly harsh to planets with Earth-like bolometric fluxes around the coolest stars.

6.2. Predictions for JWST Rocky Worlds

What does this new shoreline model predict for the atmospheres that the JWST Rocky Worlds DDT program may find? Table 1 and Figure 9 show estimated atmosphere probabilities for the 9 planned Rocky Worlds targets. Of these, GJ 3929 b has already been observed, and its atmospheric non-detection (Q. Xue et al. 2025) was included in the shoreline fit. LTT 1445Ab's bright MIRI/LRS spectrum (P. Wachiraphan et al. 2025, where we confirmed the near-zero eccentricity of the orbit) also contributed to the current shoreline, but the Rocky Worlds' $15\mu\text{m}$ photometry can probe much more tenuous CO_2 atmospheres (J. Ih et al. 2023) and could in the future flip it to $A_i = 1$. Figure 9 shows the Rocky Worlds targets span a broad range of fluxes, gravities, and host star luminosities, with motivation for such breadth emerging from predictive target optimization experiments (J. Ih et al. 2025). Here, we predict 5/9 of these Rocky Worlds targets to have atmosphere probabilities $> 50\%$, and the expected number of atmospheres (= the sum of these probabilities) to be 5.36. By spanning a range of shoreline distances (Δ_i , see Equation 3), the new Rocky Worlds observations will have strong leverage to test the predictions of this shoreline model and update its parameters, in addition to discovering what will likely be some of the easiest-to-observe rocky exoplanet atmospheres in the Universe.

6.3. Relevance for Habitable Zone Planets

Can all planets in the habitable zone retain atmospheres? Cast in terms of semimajor axis $a = \sqrt{L_*/4\pi f}$, the shoreline orbital distance scales as $a_{\text{shoreline}} \propto L_*^{(1-q)/2}$. Our inferred $q = 1.17^{+0.28}_{-0.20}$ is mostly > 1 , implying that $a_{\text{shoreline}}$ grows *outward* toward smaller stars. In contrast, the habitable zone distance necessarily shrinks inward toward smaller stars as $a_{\text{hz}} \propto L_*^{1/2}$ (generally making them easier to observe; C. H. Blake et al. 2008; P. Nutzman & D. Charbonneau 2008). Figure 10 demonstrates where these two curves intersect. For these plots, we use the mass-radius relation of Figure 1 to translate v_{esc} into planet radius R_p , and we show

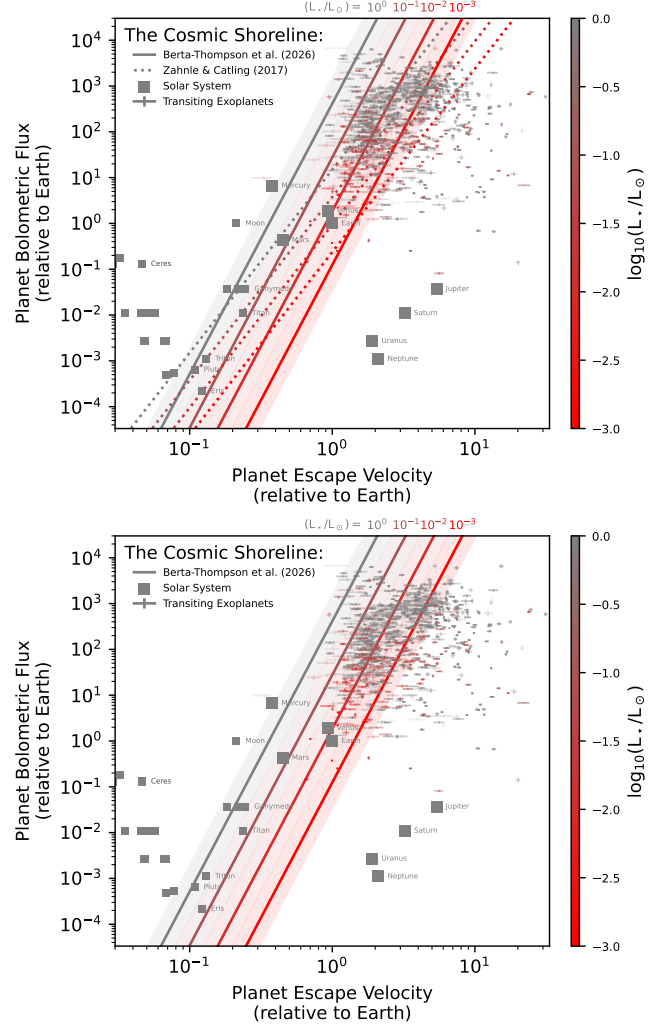


Figure 8. The inferred cosmic shoreline with all planets compressed onto a single plot, both with and without comparison to the traditional (K. J. Zahnle & D. C. Catling 2017) XUV-driven shoreline. Colors indicate host star luminosity L_* both for individual planets and for the shoreline to which they should be compared, with swaths spanning the $\pm 1w$ intrinsic logistic width of the shoreline. Plotted lines follow the equation $\log_{10}(f_{\text{shoreline}}/f_{\oplus}) = \log_{10}(f_0/f_{\oplus}) + p \log_{10}(v_{\text{esc}}/v_{\text{esc},\oplus}) + q \log_{10}(L_*/L_{\odot})$. Although we encourage future users to incorporate uncertainties by drawing samples from the parameter posteriors, the best-fit parameters used here were $\log_{10}(f_0/f_{\oplus}) = 2.62$, $p = 5.9$, $q = 1.17$, and $\ln w = -1.4$ ($</>$).

predictions for roughly Earth-size planets as well as for larger super-Earths.

The very idea of the habitable zone depends on a planet retaining an atmosphere to support a hydrological cycle and climate feedbacks. If a planet falls within the classical habitable zone but also on the dry side of the cosmic shoreline, the planet has likely lost its atmosphere, its water, and its habitability. With the

Table 1. Predicted atmosphere probabilities for JWST Rocky Worlds Targets

Planet	$\log_{10}(f/f_{\oplus})$	$\log_{10}(v_{\text{esc}}/v_{\text{esc},\oplus})$	$\log_{10}(L_{\star}/L_{\odot})$	$P(A_i = 1)$
GJ-3929 b	1.287	0.023	-1.965	$4.53 \pm 3.8\%$
LTT-1445 A c	1.066	0.048	-2.056	$10.4^{+8.3}_{-7.6}\%$
LTT-1445 A b	0.756	0.158	-2.091	$77.1^{+13}_{-14}\%$
LHS-1140 b	-0.424	0.255	-2.470	$99.3^{+0.67}_{-0.27}\%$
TOI-198 b	0.485	0.217	-1.509	$99.7^{+0.29}_{-0.26}\%$
TOI-406 c	1.251	0.099	-1.712	$43.1^{+15}_{-16}\%$
TOI-771 b	1.248	0.160	-2.260	$21.6^{+14}_{-14}\%$
HD 260655 c	1.202	0.153	-1.441	$91.8 \pm 4.6\%$
TOI-244 b	0.865	0.123	-1.651	$88.6^{+6.5}_{-6.7}\%$

NOTE—Planet inputs are calculated from the table on the JWST Rocky Worlds project website (<https://rockyworlds.stsci.edu>), retrieved 1 March 2026. Atmosphere probabilities $P(A_i = 1)$ are calculated via Equation 4, sampling from the parameter posterior distribution (but not the individual planet property uncertainties) and quoting central 68.3% confidence intervals on the predicted probability ($\langle \rangle$).

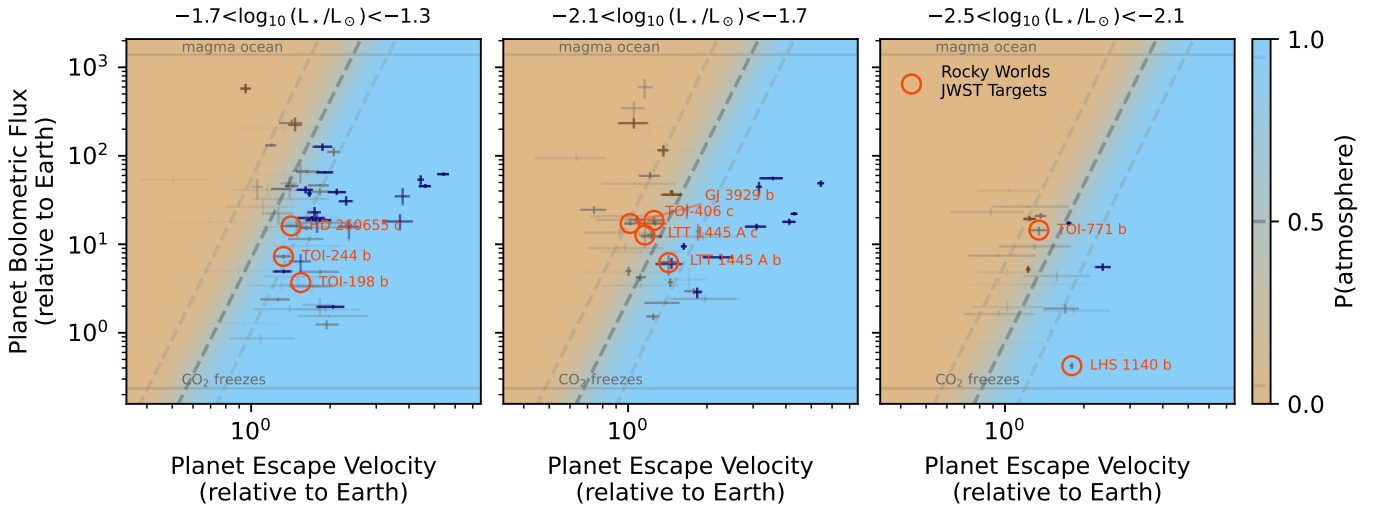


Figure 9. Cosmic shoreline predictions highlighting the JWST Rocky Worlds targets being observed in thermal emission at $15 \mu\text{m}$ with JWST/MIRI. These panels are strongly zoomed relative to Figures 2, 3, and 5 to show detail on the positions of each planet relative to the shoreline. By spanning a broad range of stellar luminosity, escape velocity, and bolometric flux, the Rocky Worlds planets will provide sensitive tests of the shoreline model proposed here and/or refinement to its parameters ($\langle \rangle$).

shoreline model presented here (and also the original from ZC17), habitable-zone planets orbiting the lowest mass M dwarfs are likely unable to retain atmospheres. Though such planets offer enormous observational advantages for transit measurements, the harsh XUV and atmospheric loss environment of low-mass stars suggests we may have more luck finding atmospheres on slightly larger planets orbiting slightly hotter stars.

7. CONCLUSIONS

In this paper, we present a probabilistic 3D cosmic shoreline model that defines the maximum bolometric

flux $f_{\text{shoreline}}$ a planet with given escape velocity v_{esc} and stellar luminosity L_{\star} can receive and still maintain a substantial atmosphere. We infer parameters for this model by fitting to exoplanets and Solar System bodies with atmospheres or global surface volatiles. We currently see no strong evidence for different shoreline parameters when we zoom in to consider only temperate atmospheres where CO_2 can exist as a gas, just larger uncertainties on the shoreline parameters.

We provide three tools to help reproduce, expand, and/or make use of the results presented in this paper:

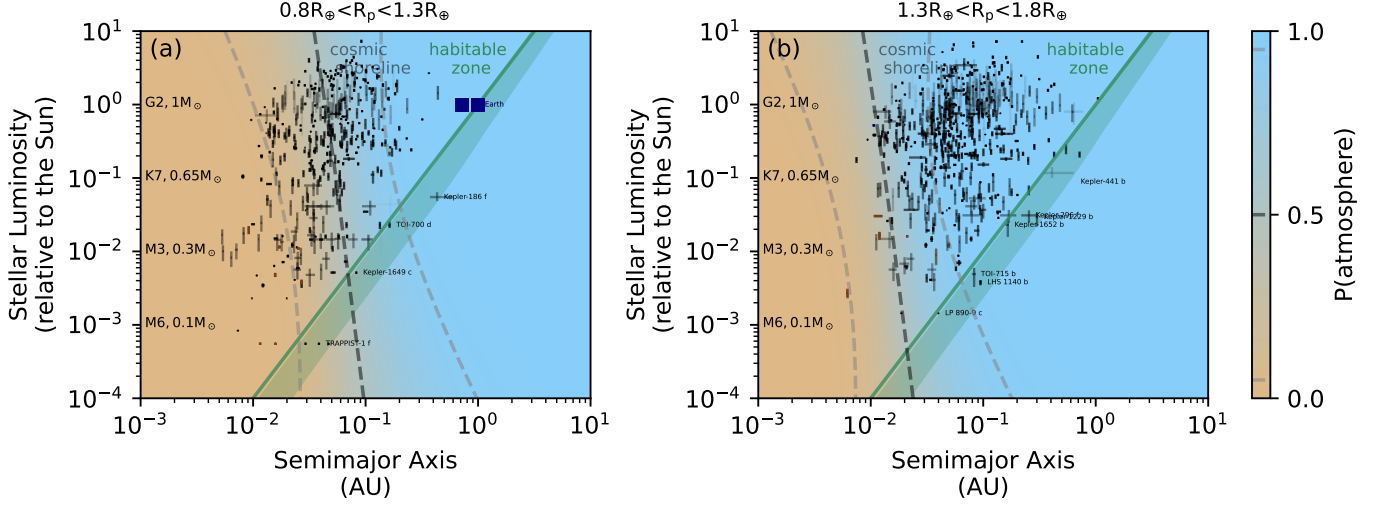


Figure 10. The cosmic shoreline model from this paper, transformed into planet semimajor axis a and planet radius R_p , and compared to liquid-water habitable zone. Approximate main-sequence spectral types and stellar masses are provided for reference. Smaller Earth-size rocky planets (a) are less able to retain atmospheres than larger super-Earths (b), such that Earth-size planets in the habitable zone of the lowest mass stars have likely lost their atmospheres (</>).

- The `exoatlas` Python code to access, filter, and visualize archival planet properties (Z. Berta-Thompson 2025), which is publicly available via `pip install exoatlas` and under review at the Journal of Open Source Software.
- `jupyter` notebooks to reproduce all paper figures and major analyses in a GitHub repository (</>).
- a `zenodo` repository containing parameter posterior samples for the main cosmic shoreline fit, as well organized planet populations, additional test posteriors, and a more expansive collection of figures and animations (Z. Berta-Thompson 2026).

The 3D shoreline presented here (Equations 2 + 4) relies on four parameters: $\log_{10}(f_0/f_{\oplus}) = 2.62^{+0.45}_{-0.31}$, $p = 5.9^{+0.61}_{-0.43}$, $q = 1.17^{+0.28}_{-0.20}$, and $\ln w = -1.40^{+0.32}_{-0.30}$. Using the multivariate posterior probability distribution of these parameters, we can predict answers to a few basic hypothetical questions about our own Solar System (</>):

- How much bigger would Mercury need to be to retain an atmosphere? Orbiting the Sun at 0.39 AU and receiving $f/f_{\oplus} = 6.7$, Mercury would need an escape velocity of at least $v_{\text{esc}}/v_{\text{esc},\oplus} = (f/f_0)^{1/p} = 0.497^{+0.047}_{-0.053}$ to have a 50% chance of having an atmosphere. By the mass-radius relation in Figure 1, this translates to about $0.478^{+0.037}_{-0.042} R_{\oplus}$, or $1.25^{+0.10}_{-0.11} \times$ its current size.
- How much hotter could Venus be before losing its atmosphere? Moving this approximately Earth-size planet with $v_{\text{esc}}/v_{\text{esc},\oplus} = 0.93$ inward to the

Sun would apparently permit it to retain significant atmosphere until it reaches the shoreline at $\log_{10}(f/f_{\oplus}) = 2.42^{+0.44}_{-0.3}$, or $a = 0.062^{+0.026}_{-0.024}$ AU. This suggests ultra-close rocky planets around FGK stars may be able to retain atmospheres, as difficult as they may be to observe.

- How much could we shrink the Sun’s mass/radius/luminosity before a habitable-zone Earth-size planet can no longer maintain any atmosphere at all? For $1R_{\oplus}$ planets with $v_{\text{esc}}/v_{\text{esc},\oplus} = 1$, the cosmic shoreline intersects with $f/f_{\oplus} = 1$ at $\log_{10}(L_*/L_{\odot}) = -2.23^{+0.18}_{-0.21}$ (or roughly M4 spectral type or $0.25 M_{\odot}$ mass). Notably, for larger $1.5R_{\oplus}$ planets with $v_{\text{esc}}/v_{\text{esc},\oplus} \approx 1.6$, this intersection extends down to $\log_{10}(L_*/L_{\odot}) = -3.28^{+0.3}_{-0.35}$ (roughly M8V spectral type or $0.09 M_{\odot}$ mass, approximately TRAPPIST-1).
- How much must we perturb planets to move them from one side of the shoreline to the other? We include an intrinsic width to the shoreline, finding that transitioning from a 95% chance of having an atmosphere to a 95% chance of not having one spans $w_{95} = 1.46^{+0.54}_{-0.38}$ dex in bolometric flux, $0.246^{+0.073}_{-0.057}$ dex in escape velocity, or $1.24^{+0.33}_{-0.26}$ dex in stellar luminosity. This intrinsic width exceeds the measurement uncertainties for most well-characterized transiting planets, so they have little effect on the inferred shoreline parameters.

Of the 9 rocky planets being observed in the JWST Rocky Worlds DDT program, we predict 5 have a $> 50\%$

chance of hosting a detectable atmosphere. We caution that the atmosphere labels in this paper are a still little fuzzy, with “no atmosphere” often really meaning “probably $\lesssim 10$ bar CO_2 ”. Rocky World’s 15 μm MIRI photometry can be sensitive to more tenuous CO_2 atmospheres than were detectable for many of the planets used here, potentially converting planets currently labeled as atmosphereless into ones with atmospheres. Other rocky exoplanet JWST programs, like the large Charting the Cosmic Shoreline (JWST-GO-7073) transmission spectroscopy program, will hopefully also add new atmosphere detections in the years to come. This model can be updated as new atmosphere constraints come in, sharpening the inferred shoreline parameters and hopefully improving its predictive and explanatory power. In the meantime, the steep slopes p and q found here imply that future searches for rocky planet atmospheres might be most fruitful for larger rocky planets (higher v_{esc}) orbiting more massive stars (higher L_*).

In this work, we attempted to capture the most important first-order inputs for long-term atmospheric evolution: the energy planets receive from their star, the strength of gravity to resist escape, and the knowledge that lower-mass stars emit more of their energy in the XUV wavelengths that matter most for escape. We assume the boundary in this 3D space between worlds with and without atmospheres is planar, with constant log-linear slopes. These are clearly rough approximations. Additional inputs surely matter, such as age, disk chemistry, dynamical history, impact and accretion history, and interior-atmosphere interactions.

Thinking of how to improve this model, the $(v_{\text{esc}}/v_{\text{esc},\oplus})^p$ term in Equation 1 could be replaced with more nuanced probabilistic functions based on atmospheric evolution models that explicitly track time-integrated sources and sinks. The $(L_*/L_\odot)^q$ term could be replaced with more precise empirical/theoretical estimates of how XUV and other drivers of atmospheric loss scale with stellar luminosity, with age, and with metallicity. But for now, the fairly broad intrinsic width w we infer for this cartoonish shoreline likely encapsulates errors in the shape of the shoreline, unmodeled hidden variables not yet included in the model, and even potentially an underlying chaotic stochasticity, where two

planets with seemingly very similar environments might have diverging atmospheric histories. Empirically disentangling a wiggly shoreline topography or the need for more dimensions from this true randomness will likely require larger sample of rocky exoplanet atmospheres.

ACKNOWLEDGMENTS

We gratefully thank Autumn Stephens, Valerie Arriero, Mirielle Caradonna, Jackson Avery, Girish Duvvuri, Sebastian Pineda, Yuta Notsu, Dave Brain, Ren e Doyon, Nicolas Cowan, Casey Brinkman, Andrew Cumming, the CU Stars and Planets Research Club, and the very thoughtful anonymous referee for conversations that improved this work. We also thank Dan Foreman-Mackey and Jake VanderPlas for pedagogical statistics blog posts that inspired some of the methods used here. This research has made use of the NASA Exoplanet Archive, which is operated by the California Institute of Technology, under contract with the National Aeronautics and Space Administration under the Exoplanet Exploration Program, as well as the planetary body archive maintained by the JPL Solar System Dynamics group. This material is based upon work supported by the National Science Foundation under Grant No. 1945633, as well as program #JWST-GO-2708 provided by NASA through a grant from the Space Telescope Science Institute, which is operated by the Association of Universities for Research in Astronomy, Inc., under NASA contract NAS 5-03127.

AUTHOR CONTRIBUTIONS

Z. Berta-Thompson planned the project, did the analyses, and wrote the manuscript. P. Wachiraphan and C. Murray contributed expertise and reviewed the manuscript.

Facilities: Exoplanet Archive, HST, JWST, Spitzer, Kepler, TESS

Software: `astropy` (Astropy Collaboration et al. 2013, 2018, 2022), `numpy` (C. R. Harris et al. 2020), `matplotlib` (J. D. Hunter 2007), `jax` (J. Bradbury et al. 2018), `numpyro` (D. Phan et al. 2019), `arviz` (R. Kumar et al. 2019), `exoatlas` (github.com/zkbt/exoatlas)

REFERENCES

- Allen, N. H., Espinoza, N., Diamond-Lowe, H., et al. 2025, *The Astronomical Journal*, 170, 240, doi: [10.3847/1538-3881/adfc51](https://doi.org/10.3847/1538-3881/adfc51)
- Astropy Collaboration, Robitaille, T. P., Tollerud, E. J., et al. 2013, *Astronomy and Astrophysics*, 558, A33, doi: [10.1051/0004-6361/201322068](https://doi.org/10.1051/0004-6361/201322068)

- Astropy Collaboration, Price-Whelan, A. M., Sipőcz, B. M., et al. 2018, *The Astronomical Journal*, 156, 123, doi: [10.3847/1538-3881/aabc4f](https://doi.org/10.3847/1538-3881/aabc4f)
- Astropy Collaboration, Price-Whelan, A. M., Lim, P. L., et al. 2022, *The Astrophysical Journal*, 935, 167, doi: [10.3847/1538-4357/ac7c74](https://doi.org/10.3847/1538-4357/ac7c74)
- August, P. C., Buchhave, L. A., Diamond-Lowe, H., et al. 2025, *Astronomy and Astrophysics*, 695, A171, doi: [10.1051/0004-6361/202452611](https://doi.org/10.1051/0004-6361/202452611)
- Bello-Arufe, A., Damiano, M., Bennett, K. A., et al. 2025, *The Astrophysical Journal*, 980, L26, doi: [10.3847/2041-8213/adaf22](https://doi.org/10.3847/2041-8213/adaf22)
- Berta-Thompson, Z. 2025, *Zkbt/Exoatlas*,
Berta-Thompson, Z. 2026, *The 3D Cosmic Shoreline for Nurturing Planetary Atmospheres*, Zenodo, doi: [10.5281/ZENODO.15858768](https://doi.org/10.5281/ZENODO.15858768)
- Blake, C. H., Bloom, J. S., Latham, D. W., et al. 2008, *Publications of the Astronomical Society of the Pacific*, 120, 860, doi: [10.1086/590506](https://doi.org/10.1086/590506)
- Boukaré, C.-É., Cowan, N. B., & Badro, J. 2022, *The Astrophysical Journal*, Volume 936, Issue 2, id.148, 9 pp., 936, 148, doi: [10.3847/1538-4357/ac8792](https://doi.org/10.3847/1538-4357/ac8792)
- Bradbury, J., Frostig, R., Hawkins, P., et al. 2018, *JAX: Composable Transformations of Python+NumPy Programs*,
- Brinkman, C. L., Weiss, L. M., Dai, F., et al. 2023, *The Astronomical Journal*, 165, 88, doi: [10.3847/1538-3881/acad83](https://doi.org/10.3847/1538-3881/acad83)
- Chaffin, M. S., Kass, D. M., Aoki, S., et al. 2021, *Nature Astronomy*, 5, 1036, doi: [10.1038/s41550-021-01425-w](https://doi.org/10.1038/s41550-021-01425-w)
- Chamberlain, J. W. 1962, *The Astrophysical Journal*, 136, 582, doi: [10.1086/147409](https://doi.org/10.1086/147409)
- Chamberlain, J. W., & Huntten, D. M. 1987, *Theory of Planetary Atmospheres. An Introduction to Their Physics Andchemistry.*, Vol. 36 (Academic Press Inc.)
- Chatterjee, R. D., & Pierrehumbert, R. T. 2024, *arXiv e-prints*, arXiv:2412.05188, doi: [10.48550/arXiv.2412.05188](https://doi.org/10.48550/arXiv.2412.05188)
- Chen, H., & Rogers, L. A. 2016, *The Astrophysical Journal*, 831, 180, doi: [10.3847/0004-637X/831/2/180](https://doi.org/10.3847/0004-637X/831/2/180)
- Chen, J., & Kipping, D. 2017, *The Astrophysical Journal*, 834, 17, doi: [10.3847/1538-4357/834/1/17](https://doi.org/10.3847/1538-4357/834/1/17)
- Chin, L., Dong, C., & Lingam, M. 2024, *The Astrophysical Journal*, 963, L20, doi: [10.3847/2041-8213/ad27d8](https://doi.org/10.3847/2041-8213/ad27d8)
- Christiansen, J. L., McElroy, D. L., Harbut, M., et al. 2025, *arXiv e-prints*, arXiv:2506.03299, doi: [10.48550/arXiv.2506.03299](https://doi.org/10.48550/arXiv.2506.03299)
- Crossfield, I. J. M., Malik, M., Hill, M. L., et al. 2022, *The Astrophysical Journal*, 937, L17, doi: [10.3847/2041-8213/ac886b](https://doi.org/10.3847/2041-8213/ac886b)
- Diamond-Lowe, H., Youngblood, A., Charbonneau, D., et al. 2021, *The Astronomical Journal*, 162, 10, doi: [10.3847/1538-3881/abfa1c](https://doi.org/10.3847/1538-3881/abfa1c)
- Dorn, C., & Lichtenberg, T. 2021, *The Astrophysical Journal*, 922, L4, doi: [10.3847/2041-8213/ac33af](https://doi.org/10.3847/2041-8213/ac33af)
- Ducrot, E., Lagage, P.-O., Min, M., et al. 2025, *Nature Astronomy*, 9, 358, doi: [10.1038/s41550-024-02428-z](https://doi.org/10.1038/s41550-024-02428-z)
- Duvvuri, G. M., Cauley, P. W., Aguirre, F. C., et al. 2023, *The Astronomical Journal*, 166, 196, doi: [10.3847/1538-3881/acfa74](https://doi.org/10.3847/1538-3881/acfa74)
- Elkins-Tanton, L. T., & Seager, S. 2008, *The Astrophysical Journal*, 685, 1237, doi: [10.1086/591433](https://doi.org/10.1086/591433)
- Erkaev, N. V., Kulikov, Yu. N., Lammer, H., et al. 2007, *Astronomy and Astrophysics*, 472, 329, doi: [10.1051/0004-6361:20066929](https://doi.org/10.1051/0004-6361:20066929)
- Esteves, L. J., De Mooij, E. J. W., & Jayawardhana, R. 2015, *The Astrophysical Journal*, 804, 150, doi: [10.1088/0004-637X/804/2/150](https://doi.org/10.1088/0004-637X/804/2/150)
- Faucher, T. J., Rackham, B. V., Ducrot, E., Stevenson, K. B., & de Wit, J. 2025, *Stellar Models Also Limit Exoplanet Atmosphere Studies in Emission*, arXiv, doi: [10.48550/arXiv.2502.19585](https://doi.org/10.48550/arXiv.2502.19585)
- Feinstein, A. D., France, K., Youngblood, A., et al. 2022, *The Astronomical Journal*, 164, 110, doi: [10.3847/1538-3881/ac8107](https://doi.org/10.3847/1538-3881/ac8107)
- Foreman-Mackey, D. 2016, *The Journal of Open Source Software*, 1, 24, doi: [10.21105/joss.00024](https://doi.org/10.21105/joss.00024)
- Foreman-Mackey, D. 2017, doi: [10.5281/ZENODO.3221477](https://doi.org/10.5281/ZENODO.3221477)
- Fortune, M., Gibson, N. P., Diamond-Lowe, H., et al. 2025, *Hot Rocks Survey III: A Deep Eclipse for LHS 1140c and a New Gaussian Process Method to Account for Correlated Noise in Individual Pixels*, arXiv, doi: [10.48550/arXiv.2505.22186](https://doi.org/10.48550/arXiv.2505.22186)
- France, K., Loyd, R. O. P., Youngblood, A., et al. 2016, *The Astrophysical Journal*, 820, 89, doi: [10.3847/0004-637X/820/2/89](https://doi.org/10.3847/0004-637X/820/2/89)
- France, K., Duvvuri, G., Egan, H., et al. 2020, *The Astronomical Journal*, 160, 237, doi: [10.3847/1538-3881/abb465](https://doi.org/10.3847/1538-3881/abb465)
- Fulton, B. J., & Petigura, E. A. 2018, *The Astronomical Journal*, 156, 264, doi: [10.3847/1538-3881/aae828](https://doi.org/10.3847/1538-3881/aae828)
- Gelman, A., & Rubin, D. B. 1992, *Statistical Science*, 7, 457, doi: [10.1214/ss/1177011136](https://doi.org/10.1214/ss/1177011136)
- Gialluca, M. T., Barnes, R., Meadows, V. S., et al. 2024, *The Planetary Science Journal*, 5, 137, doi: [10.3847/PSJ/ad4454](https://doi.org/10.3847/PSJ/ad4454)
- Greene, T. P., Bell, T. J., Ducrot, E., et al. 2023, *Nature*, 618, 39, doi: [10.1038/s41586-023-05951-7](https://doi.org/10.1038/s41586-023-05951-7)

- Gronoff, G., Arras, P., Baraka, S., et al. 2020, *Journal of Geophysical Research: Space Physics*, 125, e2019JA027639, doi: [10.1029/2019JA027639](https://doi.org/10.1029/2019JA027639)
- Grundy, W. M., Wong, I., Glein, C. R., et al. 2024, *Icarus*, 412, 115999, doi: [10.1016/j.icarus.2024.115999](https://doi.org/10.1016/j.icarus.2024.115999)
- Gupta, A., & Schlichting, H. E. 2019, *Monthly Notices of the Royal Astronomical Society*, 487, 24, doi: [10.1093/mnras/stz1230](https://doi.org/10.1093/mnras/stz1230)
- Gupta, A., & Schlichting, H. E. 2021, *Monthly Notices of the Royal Astronomical Society*, 504, 4634, doi: [10.1093/mnras/stab1128](https://doi.org/10.1093/mnras/stab1128)
- Hamano, K., Abe, Y., & Genda, H. 2013, *Nature*, 497, 607, doi: [10.1038/nature12163](https://doi.org/10.1038/nature12163)
- Hansen, J., Angerhausen, D., Quanz, S. P., et al. 2025, Detecting Atmospheric CO₂ Trends as Population-Level Signatures for Long-Term Stable Water Oceans and Biotic Activity on Temperate Terrestrial Exoplanets, arXiv, doi: [10.48550/arXiv.2505.23230](https://doi.org/10.48550/arXiv.2505.23230)
- Harris, C. R., Millman, K. J., Van Der Walt, S. J., et al. 2020, *Nature*, 585, 357, doi: [10.1038/s41586-020-2649-2](https://doi.org/10.1038/s41586-020-2649-2)
- Hoffman, M. D., & Gelman, A. 2011, arXiv e-prints, arXiv:1111.4246, doi: [10.48550/arXiv.1111.4246](https://doi.org/10.48550/arXiv.1111.4246)
- Hogg, D. W., Bovy, J., & Lang, D. 2010, arXiv e-prints, arXiv:1008.4686, doi: [10.48550/arXiv.1008.4686](https://doi.org/10.48550/arXiv.1008.4686)
- Hogg, D. W., & Foreman-Mackey, D. 2018, *The Astrophysical Journal Supplement Series*, 236, 11, doi: [10.3847/1538-4365/aab76e](https://doi.org/10.3847/1538-4365/aab76e)
- Howard, W. S., Kowalski, A. F., Flagg, L., et al. 2023, *The Astrophysical Journal*, 959, 64, doi: [10.3847/1538-4357/acfe75](https://doi.org/10.3847/1538-4357/acfe75)
- Hu, R., Demory, B.-O., Seager, S., Lewis, N., & Showman, A. P. 2015, *The Astrophysical Journal*, 802, 51, doi: [10.1088/0004-637X/802/1/51](https://doi.org/10.1088/0004-637X/802/1/51)
- Hu, R., Bello-Arufe, A., Zhang, M., et al. 2024, *Nature*, 630, 609, doi: [10.1038/s41586-024-07432-x](https://doi.org/10.1038/s41586-024-07432-x)
- Hunter, J. D. 2007, *Computing in Science & Engineering*, 9, 90, doi: [10.1109/MCSE.2007.55](https://doi.org/10.1109/MCSE.2007.55)
- Ih, J., Kempton, E. M.-R., Whittaker, E. A., & Lessard, M. 2023, *The Astrophysical Journal*, 952, L4, doi: [10.3847/2041-8213/ace03b](https://doi.org/10.3847/2041-8213/ace03b)
- Ih, J., Kempton, E. M. R., Diamond-Lowe, H., et al. 2025, doi: [10.48550/arXiv.2508.08253](https://doi.org/10.48550/arXiv.2508.08253)
- Ingersoll, A. P. 1969, *Journal of the Atmospheric Sciences*, 26, 1191, doi: [10.1175/1520-0469\(1969\)026<1191:TRGAHO>2.0.CO;2](https://doi.org/10.1175/1520-0469(1969)026<1191:TRGAHO>2.0.CO;2)
- Ingersoll, A. P. 2013, *Planetary Climates* (Princeton University Press)
- Irwin, J., Hodgkin, S., Aigrain, S., et al. 2007, *Monthly Notices of the Royal Astronomical Society*, 377, 741, doi: [10.1111/j.1365-2966.2007.11640.x](https://doi.org/10.1111/j.1365-2966.2007.11640.x)
- Ivezić, Ž., Connolly, A. J., VanderPlas, J., Gray, A., & VanderPlas, J. 2020, *Statistics, Data Mining, and Machine Learning in Astronomy: A Practical Python Guide for the Analysis of Survey Data*, updated edition edn., Princeton Series in Modern Observational Astronomy (Princeton Oxford: Princeton University Press)
- Jakosky, B. M., Grebowsky, J. M., Luhmann, J. G., et al. 2015, *Science*, 350, aad0210, doi: [10.1126/science.aad0210](https://doi.org/10.1126/science.aad0210)
- Jakosky, B. M., Brain, D., Chaffin, M., et al. 2018, *Icarus*, 315, 146, doi: [10.1016/j.icarus.2018.05.030](https://doi.org/10.1016/j.icarus.2018.05.030)
- Ji, X., Chatterjee, R. D., Coy, B. P., & Kite, E. S. 2025, The Cosmic Shoreline Revisited: A Metric for Atmospheric Retention Informed by Hydrodynamic Escape, arXiv, doi: [10.48550/arXiv.2504.19872](https://doi.org/10.48550/arXiv.2504.19872)
- Johnson, R. E., Combi, M. R., Fox, J. L., et al. 2008, *Space Science Reviews*, 139, 355, doi: [10.1007/s11214-008-9415-3](https://doi.org/10.1007/s11214-008-9415-3)
- Johnstone, C. P., Bartel, M., & Güdel, M. 2021, *Astronomy and Astrophysics*, 649, A96, doi: [10.1051/0004-6361/202038407](https://doi.org/10.1051/0004-6361/202038407)
- Johnstone, C. P., Güdel, M., Lammer, H., & Kislyakova, K. G. 2018, *Astronomy and Astrophysics*, 617, A107, doi: [10.1051/0004-6361/201832776](https://doi.org/10.1051/0004-6361/201832776)
- King, G. W., Corrales, L. R., Bourrier, V., et al. 2025, *The Astrophysical Journal*, 980, 27, doi: [10.3847/1538-4357/ada948](https://doi.org/10.3847/1538-4357/ada948)
- Kite, E. S., Fegley, B., Schaefer, L., & Gaidos, E. 2016, *The Astrophysical Journal*, 828, 80, doi: [10.3847/0004-637X/828/2/80](https://doi.org/10.3847/0004-637X/828/2/80)
- Koll, D. D. B. 2022, *The Astrophysical Journal*, 924, 134, doi: [10.3847/1538-4357/ac3b48](https://doi.org/10.3847/1538-4357/ac3b48)
- Koll, D. D. B., Malik, M., Mansfield, M., et al. 2019, *The Astrophysical Journal*, 886, 140, doi: [10.3847/1538-4357/ab4c91](https://doi.org/10.3847/1538-4357/ab4c91)
- Komabayasi, M. 1967, *Journal of the Meteorological Society of Japan*, 45, 137, doi: [10.2151/jmsj1965.45.1.137](https://doi.org/10.2151/jmsj1965.45.1.137)
- Kopparapu, R. K., Ramirez, R., Kasting, J. F., et al. 2013, *The Astrophysical Journal*, 765, 131, doi: [10.1088/0004-637X/765/2/131](https://doi.org/10.1088/0004-637X/765/2/131)
- Kreidberg, L., Koll, D. D. B., Morley, C., et al. 2019, *Nature*, 573, 87, doi: [10.1038/s41586-019-1497-4](https://doi.org/10.1038/s41586-019-1497-4)
- Krissansen-Totton, J., Wogan, N., Thompson, M., & Fortney, J. J. 2024, *Nature Communications*, 15, 8374, doi: [10.1038/s41467-024-52642-6](https://doi.org/10.1038/s41467-024-52642-6)
- Kumar, R., Carroll, C., Hartikainen, A., & Martin, O. 2019, *Journal of Open Source Software*, 4, 1143, doi: [10.21105/joss.01143](https://doi.org/10.21105/joss.01143)

- Lammer, H., Kasting, J. F., Chassefière, E., et al. 2008, *Space Science Reviews*, 139, 399, doi: [10.1007/s11214-008-9413-5](https://doi.org/10.1007/s11214-008-9413-5)
- Lammer, H., Selsis, F., Ribas, I., et al. 2003, *The Astrophysical Journal*, 598, L121, doi: [10.1086/380815](https://doi.org/10.1086/380815)
- Lammer, H., Lichtenegger, H. I., Kulikov, Y. N., et al. 2007, *Astrobiology*, 7, 185, doi: [10.1089/ast.2006.0128](https://doi.org/10.1089/ast.2006.0128)
- Leconte, J., Forget, F., Charnay, B., Wordsworth, R., & Pottier, A. 2013, *Nature*, 504, 268, doi: [10.1038/nature12827](https://doi.org/10.1038/nature12827)
- Lécuyer, C., Simon, L., & Guyot, F. 2000, *Earth and Planetary Science Letters*, 181, 33, doi: [10.1016/S0012-821X\(00\)00195-3](https://doi.org/10.1016/S0012-821X(00)00195-3)
- Lee, E. J., & Owen, J. E. 2025, *The Astrophysical Journal*, 980, L40, doi: [10.3847/2041-8213/adafa3](https://doi.org/10.3847/2041-8213/adafa3)
- Lewis, J. S., & Prinn, R. G. 1984, *Planets and Their Atmospheres : Origin and Evolution*, Vol. 33 (Academic Press Inc.)
- Lim, O., Benneke, B., Doyon, R., et al. 2023, *The Astrophysical Journal*, 955, L22, doi: [10.3847/2041-8213/acf7c4](https://doi.org/10.3847/2041-8213/acf7c4)
- Linsky, J. 2019, *Host Stars and their Effects on Exoplanet Atmospheres: An Introductory Overview*, Lecture Notes in Physics, Volume 955. ISBN 978-3-030-11451-0. Springer Nature Switzerland AG, 2019, 955, doi: [10.1007/978-3-030-11452-7](https://doi.org/10.1007/978-3-030-11452-7)
- Linsky, J. L., Fontenla, J., & France, K. 2014, *The Astrophysical Journal*, 780, 61, doi: [10.1088/0004-637X/780/1/61](https://doi.org/10.1088/0004-637X/780/1/61)
- Linsky, J. L., & Redfield, S. 2024, *Space Science Reviews*, 220, 32, doi: [10.1007/s11214-024-01064-3](https://doi.org/10.1007/s11214-024-01064-3)
- Lissauer, J. J., & De Pater, I. 2019, *Fundamental Planetary Science: Physics, Chemistry and Habitability* (Cambridge University Press), doi: [10.1017/9781108304061](https://doi.org/10.1017/9781108304061)
- Lodders, K., & Fegley, B. 1998, *The Planetary Scientist's Companion / Katharina Lodders, Bruce Fegley*.
- Lopez, E. D., & Fortney, J. J. 2014, *The Astrophysical Journal*, 792, 1, doi: [10.1088/0004-637X/792/1/1](https://doi.org/10.1088/0004-637X/792/1/1)
- Loyd, R. O. P., Shkolnik, E. L., Schneider, A. C., et al. 2021, *The Astrophysical Journal*, 907, 91, doi: [10.3847/1538-4357/abd0f0](https://doi.org/10.3847/1538-4357/abd0f0)
- Luger, R., & Barnes, R. 2015, *Astrobiology*, 15, 119, doi: [10.1089/ast.2014.1231](https://doi.org/10.1089/ast.2014.1231)
- Luger, R., Barnes, R., Lopez, E., et al. 2015, *Astrobiology*, 15, 57, doi: [10.1089/ast.2014.1215](https://doi.org/10.1089/ast.2014.1215)
- Luque, R., Coy, B. P., Xue, Q., et al. 2025, *The Astronomical Journal*, 170, 49, doi: [10.3847/1538-3881/addb40](https://doi.org/10.3847/1538-3881/addb40)
- Lustig-Yaeger, J., Meadows, V. S., & Lincowski, A. P. 2019, *The Astrophysical Journal*, 887, L11, doi: [10.3847/2041-8213/ab5965](https://doi.org/10.3847/2041-8213/ab5965)
- Mansfield, M., Kite, E. S., Hu, R., et al. 2019, *The Astrophysical Journal*, 886, 141, doi: [10.3847/1538-4357/ab4c90](https://doi.org/10.3847/1538-4357/ab4c90)
- May, E. M., MacDonald, R. J., Bennett, K. A., et al. 2023, *The Astrophysical Journal*, 959, L9, doi: [10.3847/2041-8213/ad054f](https://doi.org/10.3847/2041-8213/ad054f)
- Meier Valdés, E. A., Demory, B. O., Diamond-Lowe, H., et al. 2025, *Astronomy and Astrophysics*, 698, A68, doi: [10.1051/0004-6361/202453449](https://doi.org/10.1051/0004-6361/202453449)
- Meni-Gallardo, P., & Pallé, E. 2025, doi: [10.48550/arXiv.2508.12865](https://doi.org/10.48550/arXiv.2508.12865)
- Monaghan, C., Roy, P.-A., Benneke, B., et al. 2025, *The Astronomical Journal*, 169, 239, doi: [10.3847/1538-3881/adbe75](https://doi.org/10.3847/1538-3881/adbe75)
- Moran, S. E., Stevenson, K. B., Sing, D. K., et al. 2023, *The Astrophysical Journal*, 948, L11, doi: [10.3847/2041-8213/accb9c](https://doi.org/10.3847/2041-8213/accb9c)
- Morley, C. V., Kreidberg, L., Rustamkulov, Z., Robinson, T., & Fortney, J. J. 2017, *The Astrophysical Journal*, 850, 121, doi: [10.3847/1538-4357/aa927b](https://doi.org/10.3847/1538-4357/aa927b)
- Müller, S., Baron, J., Helled, R., Bouchy, F., & Parc, L. 2024, *Astronomy & Astrophysics*, 686, A296, doi: [10.1051/0004-6361/202348690](https://doi.org/10.1051/0004-6361/202348690)
- Murray-Clay, R. A., Chiang, E. I., & Murray, N. 2009, *The Astrophysical Journal*, 693, 23, doi: [10.1088/0004-637X/693/1/23](https://doi.org/10.1088/0004-637X/693/1/23)
- NASA Exoplanet Science Institute. 2020a, *Planetary Systems Composite Table*, IPAC, doi: [10.26133/NEA13](https://doi.org/10.26133/NEA13)
- NASA Exoplanet Science Institute. 2020b, *Planetary Systems Table*, IPAC, doi: [10.26133/NEA12](https://doi.org/10.26133/NEA12)
- Nutzman, P., & Charbonneau, D. 2008, *Publications of the Astronomical Society of the Pacific*, 120, 317, doi: [10.1086/533420](https://doi.org/10.1086/533420)
- Otegi, J. F., Bouchy, F., & Helled, R. 2020, *Astronomy & Astrophysics*, 634, A43, doi: [10.1051/0004-6361/201936482](https://doi.org/10.1051/0004-6361/201936482)
- Owen, J. E. 2019, *Annual Review of Earth and Planetary Sciences*, 47, 67, doi: [10.1146/annurev-earth-053018-060246](https://doi.org/10.1146/annurev-earth-053018-060246)
- Owen, J. E., & Jackson, A. P. 2012, *Monthly Notices of the Royal Astronomical Society*, 425, 2931, doi: [10.1111/j.1365-2966.2012.21481.x](https://doi.org/10.1111/j.1365-2966.2012.21481.x)
- Owen, J. E., & Wu, Y. 2017, *The Astrophysical Journal*, 847, 29, doi: [10.3847/1538-4357/aa890a](https://doi.org/10.3847/1538-4357/aa890a)
- Park Coy, B., Ih, J., Kite, E. S., et al. 2024, *arXiv e-prints*, arXiv:2412.06573, doi: [10.48550/arXiv.2412.06573](https://doi.org/10.48550/arXiv.2412.06573)

- Pass, E. K., Charbonneau, D., & Vanderburg, A. 2025, arXiv e-prints, arXiv:2504.01182, doi: [10.48550/arXiv.2504.01182](https://doi.org/10.48550/arXiv.2504.01182)
- Patel, J. A., Brandeker, A., Kitzmann, D., et al. 2024, *Nature*, 630, 609, doi: [10.1038/s41586-024-07432-x](https://doi.org/10.1038/s41586-024-07432-x)
- Peacock, S., Barman, T., Shkolnik, E. L., et al. 2020, *The Astrophysical Journal*, 895, 5, doi: [10.3847/1538-4357/ab893a](https://doi.org/10.3847/1538-4357/ab893a)
- Pecaut, M. J., & Mamajek, E. E. 2013, *The Astrophysical Journal Supplement Series*, 208, 9, doi: [10.1088/0067-0049/208/1/9](https://doi.org/10.1088/0067-0049/208/1/9)
- Phan, D., Pradhan, N., & Jankowiak, M. 2019, *Composable Effects for Flexible and Accelerated Probabilistic Programming in NumPyro*, arXiv, doi: [10.48550/arXiv.1912.11554](https://doi.org/10.48550/arXiv.1912.11554)
- Pierrehumbert, R. T. 2010, *Principles of Planetary Climate* (Cambridge University Press)
- Pineda, J. S., Youngblood, A., & France, K. 2021a, *The Astrophysical Journal*, 918, 40, doi: [10.3847/1538-4357/ac0aea](https://doi.org/10.3847/1538-4357/ac0aea)
- Pineda, J. S., Youngblood, A., & France, K. 2021b, *The Astrophysical Journal*, 911, 111, doi: [10.3847/1538-4357/abe8d7](https://doi.org/10.3847/1538-4357/abe8d7)
- Rackham, B. V., & de Wit, J. 2024, *The Astronomical Journal*, 168, 82, doi: [10.3847/1538-3881/ad5833](https://doi.org/10.3847/1538-3881/ad5833)
- Radica, M., Piaulet-Ghorayeb, C., Taylor, J., et al. 2025, *The Astrophysical Journal*, 979, L5, doi: [10.3847/2041-8213/ada381](https://doi.org/10.3847/2041-8213/ada381)
- Rathcke, A. D., Buchhave, L. A., de Wit, J., et al. 2025, *The Astrophysical Journal*, 979, L19, doi: [10.3847/2041-8213/ada5c7](https://doi.org/10.3847/2041-8213/ada5c7)
- Redfield, S., Batalha, N., Benneke, B., et al. 2024, arXiv e-prints, arXiv:2404.02932, doi: [10.48550/arXiv.2404.02932](https://doi.org/10.48550/arXiv.2404.02932)
- Ribas, I., Guinan, E. F., Güdel, M., & Audard, M. 2005, *The Astrophysical Journal*, 622, 680, doi: [10.1086/427977](https://doi.org/10.1086/427977)
- Richey-Yowell, T., Shkolnik, E. L., Schneider, A. C., et al. 2019, *The Astrophysical Journal*, 872, 17, doi: [10.3847/1538-4357/aafa74](https://doi.org/10.3847/1538-4357/aafa74)
- Rogers, J. G., Dorn, C., Aditya Raj, V., Schlichting, H. E., & Young, E. D. 2025, *The Astrophysical Journal*, 979, 79, doi: [10.3847/1538-4357/ad9f61](https://doi.org/10.3847/1538-4357/ad9f61)
- Rogers, L. A. 2015, *The Astrophysical Journal*, Volume 801, Issue 1, article id. 41, 13 pp. (2015)., 801, 41, doi: [10.1088/0004-637X/801/1/41](https://doi.org/10.1088/0004-637X/801/1/41)
- Sanchis-Ojeda, R., Rappaport, S., Winn, J. N., et al. 2013, *The Astrophysical Journal*, 774, 54, doi: [10.1088/0004-637X/774/1/54](https://doi.org/10.1088/0004-637X/774/1/54)
- Schaefer, L., & Fegley, B. 2009, *The Astrophysical Journal*, 703, L113, doi: [10.1088/0004-637X/703/2/L113](https://doi.org/10.1088/0004-637X/703/2/L113)
- Schaefer, L., Lodders, K., & Fegley, B. 2012, *The Astrophysical Journal*, 755, 41, doi: [10.1088/0004-637X/755/1/41](https://doi.org/10.1088/0004-637X/755/1/41)
- Schaefer, L., Wordsworth, R. D., Berta-Thompson, Z., & Sasselov, D. 2016, *The Astrophysical Journal*, 829, 63, doi: [10.3847/0004-637X/829/2/63](https://doi.org/10.3847/0004-637X/829/2/63)
- Schaller, E. L., & Brown, M. E. 2007, *The Astrophysical Journal*, 659, L61, doi: [10.1086/516709](https://doi.org/10.1086/516709)
- Seager, S. 2010, *Exoplanet Atmospheres: Physical Processes* (Princeton University Press)
- Sekiya, M., Nakazawa, K., & Hayashi, C. 1980, *Earth and Planetary Science Letters*, 50, 197, doi: [10.1016/0012-821X\(80\)90130-2](https://doi.org/10.1016/0012-821X(80)90130-2)
- Seligman, D. Z., Feinstein, A. D., Lai, D., et al. 2024, *The Astrophysical Journal*, 961, 22, doi: [10.3847/1538-4357/ad0b82](https://doi.org/10.3847/1538-4357/ad0b82)
- Shields, A. L., Meadows, V. S., Bitz, C. M., et al. 2013, *Astrobiology*, vol. 13, issue 8, pp. 715-739, 13, 715, doi: [10.1089/ast.2012.0961](https://doi.org/10.1089/ast.2012.0961)
- Sicardy, B., Tej, A., Gomes-Júnior, A. R., et al. 2024, *Astronomy & Astrophysics*, Volume 682, id.L24, 8 pp., 682, L24, doi: [10.1051/0004-6361/202348756](https://doi.org/10.1051/0004-6361/202348756)
- Singh, V., Bonomo, A. S., Scandariato, G., et al. 2022, *Astronomy and Astrophysics*, 658, A132, doi: [10.1051/0004-6361/202039037](https://doi.org/10.1051/0004-6361/202039037)
- Sivia, D. S., & Skilling, J. 2011, *Data Analysis: A Bayesian Tutorial; [for Scientists and Engineers]*, 2nd edn., Oxford Science Publications (Oxford: Oxford Univ. Press)
- Teixeira, K. E., Morley, C. V., Foley, B. J., & Unterborn, C. T. 2024, *The Astrophysical Journal*, 960, 44, doi: [10.3847/1538-4357/ad0cec](https://doi.org/10.3847/1538-4357/ad0cec)
- Teske, J. K., Wallack, N. L., Piette, A. A. A., et al. 2025, *The Astrophysical Journal*, 995, L39, doi: [10.3847/2041-8213/ae0a4c](https://doi.org/10.3847/2041-8213/ae0a4c)
- Thao, P. C., Mann, A. W., Feinstein, A. D., et al. 2024, *The Astronomical Journal*, Volume 168, Issue 6, id.297, 24 pp., 168, 297, doi: [10.3847/1538-3881/ad81d7](https://doi.org/10.3847/1538-3881/ad81d7)
- Tian, F. 2009, *The Astrophysical Journal*, 703, 905, doi: [10.1088/0004-637X/703/1/905](https://doi.org/10.1088/0004-637X/703/1/905)
- Tian, F. 2015, *Annual Review of Earth and Planetary Sciences*, 43, 459, doi: [10.1146/annurev-earth-060313-054834](https://doi.org/10.1146/annurev-earth-060313-054834)
- Van Looveren, G., Boro Saikia, S., Herbort, O., et al. 2025, *Astronomy & Astrophysics*, 694, A310, doi: [10.1051/0004-6361/202452998](https://doi.org/10.1051/0004-6361/202452998)
- Van Looveren, G., Güdel, M., Boro Saikia, S., & Kislyakova, K. 2024, *Astronomy and Astrophysics*, 683, A153, doi: [10.1051/0004-6361/202348079](https://doi.org/10.1051/0004-6361/202348079)
- VanderPlas, J. 2014, arXiv e-prints, arXiv:1411.5018, doi: [10.48550/arXiv.1411.5018](https://doi.org/10.48550/arXiv.1411.5018)

- Vehtari, A., Gelman, A., Simpson, D., Carpenter, B., & Bürkner, P.-C. 2021, *Bayesian Analysis*, 16, doi: [10.1214/20-BA1221](https://doi.org/10.1214/20-BA1221)
- Wachiraphan, P., Berta-Thompson, Z. K., Diamond-Lowe, H., et al. 2025, *The Astronomical Journal*, 169, 311, doi: [10.3847/1538-3881/adc990](https://doi.org/10.3847/1538-3881/adc990)
- Walker, J. C. G., Hays, P. B., & Kasting, J. F. 1981, *Journal of Geophysical Research: Oceans*, 86, 9776, doi: [10.1029/JC086iC10p09776](https://doi.org/10.1029/JC086iC10p09776)
- Watson, A. J., Donahue, T. M., & Walker, J. C. G. 1981, *Icarus*, 48, 150, doi: [10.1016/0019-1035\(81\)90101-9](https://doi.org/10.1016/0019-1035(81)90101-9)
- Weiner Mansfield, M., Xue, Q., Zhang, M., et al. 2024, *The Astrophysical Journal*, 975, L22, doi: [10.3847/2041-8213/ad8161](https://doi.org/10.3847/2041-8213/ad8161)
- Wilson, D. J., Froning, C. S., Duvvuri, G. M., et al. 2025, *The Astrophysical Journal*, 978, 85, doi: [10.3847/1538-4357/ad9251](https://doi.org/10.3847/1538-4357/ad9251)
- Woods, T. N., Chamberlin, P. C., Harder, J. W., et al. 2009, *Geophysical Research Letters*, 36, L01101, doi: [10.1029/2008GL036373](https://doi.org/10.1029/2008GL036373)
- Wordsworth, R., & Kreidberg, L. 2022, *Annual Review of Astronomy and Astrophysics*, 60, 159, doi: [10.1146/annurev-astro-052920-125632](https://doi.org/10.1146/annurev-astro-052920-125632)
- Wordsworth, R. D., & Pierrehumbert, R. T. 2013, *The Astrophysical Journal*, 778, 154, doi: [10.1088/0004-637X/778/2/154](https://doi.org/10.1088/0004-637X/778/2/154)
- Wright, N. J., Drake, J. J., Mamajek, E. E., & Henry, G. W. 2011, *The Astrophysical Journal*, 743, 48, doi: [10.1088/0004-637X/743/1/48](https://doi.org/10.1088/0004-637X/743/1/48)
- Wyatt, M. C., Kral, Q., & Sinclair, C. A. 2020, *Monthly Notices of the Royal Astronomical Society*, 491, 782, doi: [10.1093/mnras/stz3052](https://doi.org/10.1093/mnras/stz3052)
- Xue, Q., Bean, J. L., Zhang, M., et al. 2024, *The Astrophysical Journal Letters*, Volume 973, Issue 1, id.L8, 14 pp., 973, L8, doi: [10.3847/2041-8213/ad72e9](https://doi.org/10.3847/2041-8213/ad72e9)
- Xue, Q., Zhang, M., Coy, B. P., et al. 2025, *The Astrophysical Journal*, 995, L52, doi: [10.3847/2041-8213/ae2098](https://doi.org/10.3847/2041-8213/ae2098)
- Young, L. A., Kammer, J. A., Steffl, A. J., et al. 2018, *Icarus*, Volume 300, p. 174-199., 300, 174, doi: [10.1016/j.icarus.2017.09.006](https://doi.org/10.1016/j.icarus.2017.09.006)
- Zahnle, K. 1998, *Origins*, 148, 364
- Zahnle, K. J., & Catling, D. C. 2017, *The Astrophysical Journal*, 843, 122, doi: [10.3847/1538-4357/aa7846](https://doi.org/10.3847/1538-4357/aa7846)
- Zeng, L., & Jacobsen, S. B. 2024, *Icarus*, 414, 116033, doi: [10.1016/j.icarus.2024.116033](https://doi.org/10.1016/j.icarus.2024.116033)
- Zeng, L., Jacobsen, S. B., Hyung, E., et al. 2021, *The Astrophysical Journal*, 923, 247, doi: [10.3847/1538-4357/ac3137](https://doi.org/10.3847/1538-4357/ac3137)
- Zhang, M., Hu, R., Inglis, J., et al. 2024, *The Astrophysical Journal*, 961, L44, doi: [10.3847/2041-8213/ad1a07](https://doi.org/10.3847/2041-8213/ad1a07)
- Zieba, S., Zilinskas, M., Kreidberg, L., et al. 2022, *Astronomy and Astrophysics*, 664, A79, doi: [10.1051/0004-6361/202142912](https://doi.org/10.1051/0004-6361/202142912)
- Zieba, S., Kreidberg, L., Ducrot, E., et al. 2023, *Nature*, 620, 746, doi: [10.1038/s41586-023-06232-z](https://doi.org/10.1038/s41586-023-06232-z)